The Journal of Neuroscience, October 15, 2001, *21*(20):7954–7968

Myr 8, A Novel Unconventional Myosin Expressed during Brain Development Associates with the Protein Phosphatase Catalytic Subunits 1α and 1γ1

Krishna G. Patel, Changdan Liu, Patricia L. Cameron, and Richard S. Cameron

Section of Neurobiology, Institute of Molecular Medicine and Genetics, Medical College of Georgia, Augusta, Georgia, 30912-3175

Directed neuronal, astroglial, and oligodendroglial cell migrations comprise a prominent feature of mammalian brain development. Because molecular motor proteins have been implicated in a wide spectrum of processes associated with cell motility, we initiated studies to define the pool of myosins in migrating cerebellar granule neurons and type-1 neocortical astrocytes. Our analyses identified two isoforms of a novel unconventional myosin, which we have cloned, sequenced, and designated myr 8a and 8b (eighth unconventional myosin from rat). Phylogenetic analysis indicates that myr 8 myosins comprise a new class of myosins, which we have designated class XVI. The head domain contains a large N-terminal extension composed of multiple ankyrin repeats, which are implicated in mediating an association with the protein phosphatase 1 (PP1) catalytic subunits 1α and 1γ. The motor domain is followed by a single putative light-chain binding domain. The tail domain of myr 8a is comparatively short with a net positive charge, whereas the tail domain of myr 8b is extended, bears an overall neutral charge, and reveals several stretches of polyproline residues. Neither the myr 8a nor the myr 8b sequence reveals α-helical coiled-coil motifs, suggesting that these myosins exist as monomers. Both immunoblot and Northern blot analyses indicate that myr 8b is the predominant isoform expressed in brain, principally at developmental time periods. The structural features and restricted expression patterns suggest that members of this novel class of unconventional myosins comprise a mechanism to target selectively the protein phosphatase 1 catalytic subunits 1α and/or 1γ in developing brain.

Key words: unconventional myosins; cytoskeleton; nervous system; brain development; neuronal migration; astrocytes

Directed migration of neuronal, astroglial, and oligodendroglial cells comprises a prominent feature of mammalian brain development. In the developing neocortex, considerable numbers of neurons exit the cell cycle within the ventricular zone and subsequently initiate an active cell movement along a scaffolding of radial glial cell processes to settle in the cortical plate (Sidman and Rakic, 1973; Rakic, 1990; Hatten, 1999). A lesser population of cortical neurons arise in either the ventricular zone or in subcortical structures and reach the cortex by initially traversing long distances in a nonradial or tangential manner (O'Rourke et al., 1997; Wichterle et al., 1997; Zhu et al., 1999). After reaching the appropriate destination, neurons elaborate dendritic arbors and extend axonal processes that migrate in a highly directed manner to find the appropriate synaptic partner (Tanaka and Sabry, 1995; Suter and Forscher, 1998; Andersen and Bi, 2000). Similarly, the majority of astroglial and oligodendroglial cells take residence throughout the neocortex subsequent to migration from the proliferative subventricular zone (Levison and Goldman, 1993; Zerlin et al., 1995; Kakita and Goldman, 1999).

Much is known about the cell surface receptors and associated signal transduction cascades that modulate cytoskeletal organization underlying cell movement (Lauffenburger and Horwitz, 1996; Mitchison and Cramer, 1996; Heidemann and Buxbaum, 1998; Song and Poo, 2001). Myosin proteins comprise a superfamily of actin-based motor proteins that have been implicated in a wide spectrum of processes associated with motile events (Mermall et al., 1998). Members of all classes of mammalian myosins have been detected in the nervous system, and mutations in several have been implicated in human neural diseases (Avraham et al., 1995; Gibson et al., 1995; Weil et al., 1995, 1997; Liu et al., 1997a,b; Pastural et al., 1997; Probst et al., 1998; Wang et al., 1998). To further elucidate the role of myosins in the process of neuronal cell migration, we initiated studies to define the pool of myosins in migrating cerebellar granule neurons and type-1 neocortical astrocytes.

In the present study, we have cloned and sequenced two novel unconventional myosin isoforms, myr 8a and myr 8b (eighth unconventional myosin from rat), that comprise the founding members of a new class of myosins, which we have designated class XVI. The head domain of myr 8 myosins contains an N-terminal extension composed of multiple ankyrin repeats, which biochemical evidence implicates in binding the protein phosphatase 1 (PP1) catalytic subunits 1α and 1γ. Immunoblot and Northern blot analyses reveal that myr 8b is the principal isoform expressed in brain. Myr 8b-immunoreactivity distributes in a punctate manner throughout the cell body and extended processes of both neuronal and astroglial cells in primary culture. In the developing cerebellum, myr 8b-immunoreactivity localizes predominantly to granule neurons located in the deeper portion of the external granule cell layer, a location where granule neu-

Received April 23, 2001; revised Aug. 3, 2001; accepted Aug. 3, 2001.

This research was supported by the National Institutes of Health, National Institute of Neurological Disease and Stroke Grant NS34763 to R.S.C. We thank the Protein and Molecular Biology Core Facility at Medical College of Georgia for DNA sequencing and peptide synthesis, Dr. J. Felsenstein (University of Washington) for advice in bootstrapping analyses, and Dr. R. E. Cheney (University of North Carolina) for constant enthusiasm and discussion and review of this manuscript.

Correspondence should be addressed to Richard S. Cameron, Institute of Molecular Medicine and Genetics, Medical College of Georgia, Augusta, GA 30912-3175. E-mail: rcameron@mail.mcg.edu.

rons initiate neurite extension and begin the process of neuronal migration. The structural features and restricted expression patterns suggest that this novel unconventional myosin comprises a mechanism in developing brain to target selectively the protein phosphatase 1 catalytic subunits 1α and 1γ.

MATERIALS AND METHODS

Materials. Female adult and timed-pregnant Sprague Dawley rats were obtained from Harlan (Indianapolis, IN). Postnatal animals were killed by decapitation under deep ether anesthesia. All animal use protocols were reviewed and approved by the Committee on Animal Use in Research and Education at the Medical College of Georgia. Polyclonal antiserum directed against multiple (1α, 1β, 1γ, 2A, 2B, and X – sc-443) and individual protein phosphatase catalytic subunits (1α – sc-6104, 1β – sc-6107, 1γ – sc-6108, and 2A – sc-6110) were purchased from Santa Cruz Biotechnology (Santa Cruz, CA), and polyclonal antibodies developed against actin (A2066) were obtained from Sigma (St. Louis, MO). All other supplies were obtained as indicated or were from general distributors. All images were scanned into and edited with Adobe Photoshop.

Primary cultures of astrocytes and neurons. Primary cultures of type 1 astrocytes were prepared from <24 hr neonatal rat cerebral cortices as described (Levison and McCarthy, 1991; Cameron and Rakic, 1994). Cell cultures were maintained in minimal essential medium (Earle's salts) containing 15% newborn calf serum (Life Technologies/BRL, Gaithersburg, MD) at 37°C in a humidified atmosphere of 5% CO_2. For microscopic studies, type 1 astrocytes were replated on untreated cover glasses. Cerebellar granule neurons were isolated from postnatal day 10 rat cerebella by velocity centrifugation in Percoll (Pharmacia, Piscataway, NJ) and maintained in minimal essential medium (Earle's salts) containing 1% fetal calf serum, 1% HL-1 (BioWhittaker, Walkersville, MD), 10 mM HEPES, pH 7.4, and 10 mM KCl, at 37°C in a humidified atmosphere of 5% CO_2 for 24–48 hr (Hatten, 1985; Cameron and Rakic, 1994). Primary hippocampal neurons were prepared from hippocampi of embryonic day 18 rat embryos as described (Cameron et al., 1991; Goslin and Banker, 1991) and maintained in minimal essential medium (Earle's salts) containing 1% fetal calf serum, 1% HL-1, and 10 mM HEPES, pH 7.4, at 37°C in a humidified atmosphere of 5% CO_2 for 48 hr. Both cerebellar granule and hippocampal neurons were plated on poly-L-lysine (0.25 mg/ml in 100 mM sodium borate, pH 8.4)-coated glass coverslips ($1–2 \times 10^4$ cells/cm^2).

PCR-based screen for the identification of myosin sequences. Total RNA was extracted from primary cultures of type 1 astrocytes and isolated cerebellar granule neurons using TRIzol reagent (Life Technologies). Oligo-dT-primed first-strand cDNAs were generated from total RNA using the cDNA cycle kit (Invitrogen, Carlsbad, CA). PCR amplification of cDNAs was performed using *Taq* polymerase (Stratagene, La Jolla, CA) and degenerate primers (Life Technologies) corresponding to conserved sequences of known rat myosins (Bement et al., 1994a,b), sense primer [5′-GGIGA(A/G)(A/T)(G/C)IGGIGCIGGIAA(A/G)AC-3′] and antisense primer [5′-GT(C/T)TTIGC(A/G)TTICC(A/G)AAIGC-(C/T)TC)-3′], with the following conditions: 94°C × 2 min; 40 cycles of 94°C × 1 min, 45°C × 1 min, 62°C × 3 min; 72°C × 10 min. PCR products were cloned into pBluescript T vector and transformed into XL-1 Blue bacteria using electroporation. The isolated DNA clones were reamplified by PCR (conditions as above), subjected to single restriction enzyme digestion using *Hae*III, Fnu 4H1, and *Sca*I (New England Biolabs, Beverly, MA), and resolved by PAGE to group clones by restriction enzyme fragment patterns. Plasmid DNA of clones selected from each group were purified using the Wizard kit (Promega, Madison, WI) and sequenced to determine the myosin isoforms represented for each restriction enzyme fragment pattern. Sequencing was performed using an ABI PRISM 377 automated DNA sequencer with XL upgrade (Perkin Elmer, Foster City, CA) by the Molecular Biology Core Facility at the Medical College of Georgia and analyzed using the Wisconsin Package Version 10.0, Genetics Computer Group (Madison, WI).

cDNA library screening. Random-primed ^{32}P-labeled (5′-α-[^{32}P] deoxycytosine triphosphate; Amersham, Piscataway, NJ) probe 1, nucleotide (nt) 1705–2220, was used for the initial screen of a custom-made oligo-dT-primed cDNA library (Stratagene) generated from primary cultures of type 1 astrocytes. This probe did not overlap with any of the highly conserved domains of the myosin superfamily. Hybridization-positive phages were purified, and inserts were rescued by helper-phage-mediated excision. Plasmid DNA was purified using a Wizard kit (Promega) and sequenced in both directions using multiple internal primers. Additional library screens used probes representing sequences in clone 4 located further downstream of probe 1: probe 2, nucleotides 2788–3237; probe 3, nucleotides 3436–3675. Identification of clones 8 and 18 was performed using probe 4, which was generated by PCR amplification using the KIAA0865 specific antisense primer as described below for PCR amplification of myr 8 isoforms. Probe 4 represents nucleotides 3905–4600 of the myr 8b sequence.

Northern blot analyses. Total RNA was extracted from primary cultures of type 1 astrocytes and rat tissues using TRIzol reagent (Life Technologies). Poly(A) RNA was isolated from total RNA using PolyATtract mRNA Isolation Systems (Promega). RNA samples (15 μg total RNA or 2.5 μg poly(A) RNA) and RNA size standards (Life Technologies) were separated on GTG Agarose (FMC, Rockland, ME)/formaldehyde gels and transferred to Gene Screen membranes (DuPont/NEN, Boston, MA). Nylon membranes were prehybridized overnight at 65°C in Church buffer (Church and Gilbert, 1984) and hybridized with the random-primed ^{32}P-labeled (5′-α-[^{32}P] deoxycytosine triphosphate; Amersham) cDNA probe (probe 1, 2, or 3, see above) overnight in the same buffer. After hybridization, membranes were washed with 2× SSC/0.1% SDS at room temperature, 0.1× SSC/0.1% SDS at 65°C, and then exposed to Hyperfilm MP (Amersham). Nucleotide sequence for probes 1, 2, 3, and 4 are described above. Probe 5 represents nucleotides 4110–4771, which correspond to the sequence within the tail domain that is unique to the myr 8b isoform.

PCR amplification of myr 8 isoforms. PCR amplification of cerebellar granule neuron cDNA was performed using *Taq* polymerase with a common sense primer (5′-CTCCACCCAAGCCAAAGAGG-3′) and either an antisense primer unique to the 3′-untranslated region of myr 8a (5′-ACCAGAACCCAGCCCATGA-3′) or an antisense primer unique to the KIAA0865 sequence (5′-AGGCGGGGGAGCAGGTGAC-3′) with the following PCR conditions: (1) 94°C × 2 min; 40 cycles of 94°C × 1 min, 55°C × 1 min, 72°C × 2 min; 72°C × 10 min with the myr 8 antisense primer; or (2) 94°C × 2 min; 40 cycles of 94°C × 1 min, 45°C × 1 min, 62°C × 3 min; 72°C × 10 min with the KIAA0865 antisense primer.

Polyclonal antibody development. New Zealand White rabbits were bled before immunization to obtain preimmune serum. A peptide sequence located in the tail domain of myr 8b (CSRDEPSSSEMASETQDRNANNHG) was synthesized by the Protein and Molecular Biology Core Facility (Medical College of Georgia) and conjugated to keyhole limpet hemocyanin using the Sulfhydral Imject Activated Immunogen Conjugation Kit (Pierce, Rockford, IL). The region corresponding to the N-terminal domain upstream of the ankyrin repeats domain (nucleotides 43–195; amino acids 2–52; 6199 Da) was amplified by PCR using *Taq* polymerase and ligated into the pCR T7/NT-TOPO vector (Invitrogen). Constructs were sequenced to verify sequence accuracy and correct insert orientation. Selected clones were transformed into BL21(DE3) pLys bacteria, and the expression of the fusion protein was induced by isopropylthio-β-D-galactoside. The expressed polypeptide was semipurified using nickel affinity column chromatography and purified protein obtained by electroelution from SDS-acrylamide gels (Hunkapiller et al., 1983) after copper staining (Lee et al., 1987). Immunogen (conjugated peptide or the recombinant fusion protein) was suspended in PBS (10 mM sodium phosphate, 150 mM NaCl, pH 7.4) and emulsified with Freund's adjuvant (complete for initial injection; incomplete for booster injections). Affinity purification of the peptide antibodies was performed with the SulfoLink kit following the manufacturer's protocol (Pierce).

Indirect immunofluorescence. Isolated cerebellar granule neurons, hippocampal neurons, and type 1 astrocytes cell cultures were rinsed with minimal essential media and fixed with 4% formaldehyde (freshly prepared from paraformaldehyde) in 120 mM sodium phosphate, pH 7.4 (room temperature, 20 min). For localizing antigens in postnatal tissues, rats were perfused transcardially with 4% paraformaldehyde under deep ether anesthesia, and brains and tissues of interest dissected out and fixation was continued for an additional 3 hr (4°C). Tissues were infiltrated with 12, 16, and 20% sucrose in 120 mM sodium phosphate, pH 7.4. For preparation of frozen sections, tissue samples were infiltrated with Tissue Tek compound (Miles Laboratories, Naperville, IL) at 4°C for 60 min and then frozen in liquid nitrogen-cooled isopentane. Indirect immunofluorescence analyses for cells and frozen tissue sections were performed as described (Cameron et al., 1997). The distribution of bound antibodies was visualized by use of secondary antibodies: Cy-3-conjugated goat α-rabbit IgG antibodies or Cy-3-conjugated rabbit α-mouse IgGs antibodies (Jackson ImmunoResearch Laboratories, West

Grove, PA). Control experiments with secondary antibodies alone or in the presence of the relevant peptide revealed no immunofluorescence. Coverslips were mounted in a freshly prepared solution of 10 mM sodium phosphate, pH 7.4, 150 mM NaCl, 70% glycerol, and 1 mg/ml *p*-phenylenediamine. Cells were viewed through a Zeiss Axiophot microscope equipped with epifluorescent optics and photographed using Kodak T-max 100 film.

Myr 8 antibody–Protein G Sepharose. Two milligrams of affinity-purified myr 8b antibodies were coupled to Protein G Sepharose 4 Fast Flow (Pharmacia) and cross-linked using dimethylpimelimidate (Schneider et al., 1982). For antigen preparation, postnatal day 10 cerebella were disrupted in a Brendler glass–Teflon pestle homogenizer in 250 mM sucrose supplemented with 20 mM Tris, 2 mM EDTA, 2 mM EGTA, 1 mM dithiothreitol, 1 mM sodium vanadate, 0.4 mM phenylmethylsulfonyl fluoride, and 2 μg/ml each of pepstatin, leupeptin, and antipain, pH 7.4. Centrifugation (1000 × *g* for 10 min) yielded a postnuclear supernatant, which after subsequent centrifugation (100,000 × *g* for 60 min) generated a crude cytoskeletal/membrane fraction. The crude sediment was solubilized in homogenate medium containing 1% Triton X-100 (120 min, 4°C) followed by centrifugation (12,500 × *g* for 15 min). The detergent soluble lysate was incubated with myr 8b-Sepharose beads (overnight at 4°C), and isolated proteins were processed for immunoblot analyses.

PAGE and immunoblotting. For one-dimensional SDS-PAGE-immunoblot analyses, reduced protein samples (40 mM dithiothreitol) were resolved in 5, 8, or 12.5% acrylamide gels in Laemmli (1970) buffer system. Protein was determined using the bicinchoninic assay (Pierce) with bovine serum albumin as a standard. Fractionated polypeptides were transferred electrophoretically to nitrocellulose according to the procedure of Towbin et al. (1979). Immunoblots were incubated in blocking buffer (5% nonfat dry milk, 10 mM Tris, 150 mM NaCl, pH 7.5) for 60 min and subsequently overnight in blocking buffer containing primary antiserum (1 μg/ml). For goat and mouse primary antibodies, immunoblots were incubated in blocking buffer containing a bridge antibody, either rabbit α-goat or rabbit α-mouse affinity-purified antibodies, respectively (Jackson ImmunoResearch). Bound antibodies were detected using iodinated goat α-rabbit IgG (0.5 μCi/ml, 90 min). Immunoblots were exposed to Amersham Hyperfilm at −70°C with intensifying screen for 24–72 hr. For myr 8 immunoblots, bound primary antibodies were detected using peroxidase-coupled goat α-rabbit IgG (Jackson ImmunoResearch) with visualization by enhanced chemiluminescence (DuPont/NEN).

Actin sedimentation assay. Actin cosedimentation assays were performed as described by Cheney and colleagues (Berg et al., 2000). Postnatal day 8 brain was homogenized (10% w/v) by 10 passes in a Brendler glass–Teflon pestle homogenizer (1200 rpm) in medium containing 20 mM 3-(*N*-morpholino) propane sulfonic acid (MOPS), pH 7.4, 75 mM KCl, 2.5 mM $MgCl_2$, 1 mM EGTA, 1 mM dithiothreitol, 0.4 mM phenylmethylsulfonyl fluoride, 0.5 mM ATP, and 5 μg/ml each of antipain, leupeptin, pepstatin A, and aprotinin, and a supernatant fraction obtained by centrifugation (100,000 × *g* for 15 min, 4°C; Beckman Type 60 ti rotor). Supernatant samples (100 μg protein) were supplemented with 50 μg human platelet non-muscle actin (Cytoskeleton, Denver, CO) and 50 mM glucose in the presence or absence of 0.5 U hexokinase (St. Louis, MO). After incubation (15 min at 25°C), centrifugation (128,000 × *g* for 22 min, 4°C; Beckman TLA-100.3 rotor) yielded a supernatant and a pellet that were collected, resolved by SDS-PAGE, and processed for immunoblot analysis using affinity-purified antibodies to the N-terminal domain of myr 8b.

Distribution of myr 8b by cell fractionation. For subcellular fractionation, postnatal day 8 brains were minced, resuspended in 250 mM sucrose supplemented with 20 mM MOPS, pH 7.4, 75 mM KCl, 2.5 mM $MgCl_2$, 1 mM EGTA, 1 mM dithiothreitol, 0.4 mM phenylmethylsulfonyl fluoride, and 5 μg/ml each of antipain, leupeptin, pepstatin A, and aprotinin, in the presence and absence of 0.5 mM ATP, and homogenized (10% w/v) by 10 passes in a Brendler glass homogenizer (1200 rpm). Sequential velocity sedimentation [1000 × *g* for 10 min, 4°C (Beckman GH-3.8 rotor); 10,000 × *g* for 15 min, 4°C (Beckman Type 60 ti rotor); 100,000 × *g* for 60 min, 4°C (Beckman Type 60 ti rotor)] yielded nuclear, mitochondrial, microsomal, and cytosolic fractions, respectively. Type 1 astrocytes were processed identically except that cells were disrupted by 10 passes in a ball-bearing type homogenizer. Proteins were resolved by SDS-PAGE and processed for immunoblot analysis using affinity-purified antibodies to the N-terminal domain of myr 8b. Quantification of chemiluminescent signal was performed using Kodak Image Station 440_{CF} software (DuPont/NEN) and ^{125}I-signal on a PhosphoImager (Molecular Dynamics, Sunnyvale, CA). Recoveries of protein and myr 8b immunoreactivity are based on the values obtained for the preceding fraction and ranged between 85 and 112%. Percentage distribution is relative to the total homogenate, which represents the sum of the nuclear pellet and postnuclear supernatant.

For determination of the distribution of myr 8b protein by immunoblot analysis, tissues obtained from postnatal day 10 rats were minced, resuspended in 250 mM sucrose supplemented with 20 mM MOPS, pH 7.4, 75 mM KCl, 2.5 mM $MgCl_2$, 1 mM EGTA, 1 mM dithiothreitol, 0.4 mM phenylmethylsulfonyl fluoride, 5 μg/ml each of antipain, leupeptin, pepstatin A, and aprotinin, and homogenized (10% w/v) by 10 passes in a Brendler glass homogenizer (1200 rpm). Postnuclear supernatants were prepared by low-speed centrifugation (600 × *g* for 10 min, 4°C; Beckman GH-3.8 rotor), and proteins were resolved by SDS-PAGE and processed for immunoblot analysis using affinity-purified antibodies to the N-terminal domain of myr 8b.

RESULTS

Identification of myosin classes in astrocytes and migrating neurons

To identify the myosin motors that could participate in neuronal cell migration, cDNAs were prepared from migrating cerebellar granule neurons and type 1 astrocytes, and PCR amplifications were performed using degenerate primers that corresponded to highly conserved sequences within the motor domain of known rat myosins (Bement et al., 1994a,b). To differentiate the myosins represented in the amplified pool of heterogeneous 180 bp fragments, restriction enzyme digests of individual clones were resolved by acrylamide gel electrophoresis and grouped according to restriction enzyme fragment patterns. Representative clones from each group were sequenced, and the myosin class was assigned by homology to known myosins. As demonstrated previously for other vertebrate cell types (Bement et al., 1994a,b; Solc et al., 1994), isoforms of most mammalian myosin classes were present in both astrocytes and neurons, although smooth muscle myosin appeared unique to astrocytes and myr 1 myosin appeared unique to cerebellar granule neurons (Table 1). Also identified were myosin isoforms that, although characterized in other mammalian cells, have not been described in rat, e.g., a class X myosin (78% identity to *Bos taurus*) and a class VI myosin (85% identity to human). Additionally, a sequence was present in astrocytes and cerebellar granule neurons that was not homologous to any known myosins outside of the shared conserved myosin motifs defined by the primers (Table 1).

Identification and characterization of the myr 8a sequence

To obtain the full-length sequence for this novel myosin, a cDNA probe (probe 1), generated from the sequence that did not overlap with any of the highly conserved domains present within the myosin protein family, was used for hybridization screening of an oligo-dT-primed Uni-ZAP custom cDNA library prepared from primary cultures of type 1 astrocytes. Sequencing of positive clones, performed through primer walking in both the 5′ and 3′ direction, revealed that one clone (clone 4) contained a ~4150 bp insert. Nucleotide and deduced amino acid sequences of clone 4 cDNA, which comprises myr 8a, are available from GenBank/European Molecular Biology Laboratory (EMBL)/DNA Data Bank of Japan (accession no. AF209114). The first methionine (nt 40–42) located within a consensus Kozak sequence (Kozak, 1991) is followed by a continuous open reading frame of 3969 base pairs, which predicts a 1322 amino acid polypeptide. The open reading frame also displays a stop codon (nt 4006–4008) and a consensus polyadenylation sequence (AATAAA, nt 4122–

Table 1. Spectrum of myosin isoforms detected in cerebellar granule neurons and astrocytes

Class of myosins	Percentage composition		Homolog accession no.
	Astrocytes	Neurons	
Class I			
Myr 1	0	3.2	x68199
Myr 2	6.5	1.0	x74800
Myr 3	38	25.5	x74815
Myr 3 isoform	2.4	5.0	x97650
Class II			
Nonmuscle			
Heavy chain A	43.4	16.0	U15764
Nonmuscle			
Heavy chain B*	1.6	6.0	M69181
Smooth muscle	1.6	0	S61948
Class VI			
Human VI*	0.8	3.0	U90236
Class IX			
Myr 5	0.8	1.0	x77609
Myr 7	1.6	12.7	AJ001713
Class X			
Bos taurus X*	0.8	2.0	U55042
Novel sequence	1.6	22.0	

The frequency of the myosin isoforms detected in clones obtained from cerebellar granule neurons (93 clones) and astrocytes (122 clones) is shown as a percentage of the total per cell type. The sequences from individual clones of the 180 bp PCR fragments were assigned to known myosin classes on the basis of homology using FASTA and BLAST searches of GenBank and EMBL/PIR/SWISSPROT data bases (Altschul et al., 1997). Asterisks indicate homology determination from species other than rat.

4127) located 17 nucleotides upstream of the poly(A) tail, thereby indicating that the 3′ coding sequence is complete. Multiple hybridization screens performed using probe 1, as well as multiple alternative probes, revealed additional positive clones that shared overlapping sequence with clone 4, but these clones were considerably smaller in size. Sequence comparisons to other known myosins revealed that the clone 4 sequence contained several motifs characteristic of myosins, including an ATP binding site (GERGSGKT, amino acids 497–504) and an actin binding site (SPHFILCVKPN, amino acids 1034–1044) (Bement et al., 1994a; Hasson and Mooseker, 1994; Mooseker and Cheney, 1995). Additionally, an aspartate residue is located 16 amino acids upstream from the conserved DLLAK motif (amino acids 738–742) within the motor domain. Thus, the myr 8a sequence conforms to the TEDS rule, implying that activation of this myosin is independent of head domain phosphorylation (Bement and Mooseker, 1995; Sokac and Bement, 2000). The N-terminal sequence located upstream of the ATP binding site reveals an array of eight ankyrin/ankyrin-like repeats (Fig. 1), which bear ~30% identity to the ankyrin repeats described for the large targeting subunit of myosin phosphatase (Chen et al., 1994; Shimizu et al., 1994; Fujioka et al., 1998). Immediately preceding the first ankyrin repeat is the motif (KVRF), which is conserved in all type 1 protein phosphatase regulatory subunits (PPIc binding motif consensus R/K-V/I-X-F) and is thought to be important for mediating the interaction with the protein phosphatase type 1 catalytic subunit (Egloff et al., 1997; Hirano et al., 1997; Johnson et al., 1997). Additionally, a potential protein kinase C phosphorylation site located at amino acid 53 (SQK) correlates to the phosphorylation site located at amino acid 34 (threonine) of the large targeting subunit of myosin phosphatase (Hartshorne, 1998). The putative neck domain contains a single region (CQKVIRGFLARQ, amino acids 1153–1164) similar to the IQ consensus sequence (IqxxxRGxxxRK), a region predicted to serve as the calmodulin/light-chain binding site (Mooseker and Cheney, 1995; Houdusse et al., 1996). The C-terminal tail of myr 8a, which is relatively short when compared with other myosins, comprises 158 amino acids. The tail domain has a net positive charge with a pI of 9.6, contains a short proline-rich region, and is not predicted to display extensive α-helical coiled-coil structure. We have designated this myosin as myr 8a (eighth unconventional myosin from rat, isoform a) according to the convention of Bähler and colleagues for naming rat myosins (Ruppert et al., 1993; Bähler et al., 1994; Reinhard et al., 1995; Stöffler et al., 1995; Chieregatti et al., 1998).

In comparison with known myosins, the myr 8a sequence revealed low identity to numerous myosins of multiple classes, ~30 and 50% at the amino acid and nucleotide levels, respectively. The regions of identity laid only within the head domain and correlated to the presence of conserved motor motifs, e.g., ATP and actin binding sites. However, the myr 8a sequence displayed 78% amino acid and 79% nucleotide identity to the cDNA clone KIAA0865 (GenBank accession no. AB020672) isolated from human brain (Nagase et al., 1998). Alignment of myr 8a and KIAA0865 sequences revealed that the consensus start site indicated for the KIAA0865 sequence predicted a protein that contained the actin binding site and the IQ motif but lacked the consensus ATP binding sequence characteristic of all myosins. Because the stop codon located in myr 8a/clone 4 was absent in the KIAA0865 cDNA clone, the open reading frame of KIAA0865 extended in the 3′ direction for an additional 1590 base pairs. The deduced amino acid sequence comprising the extended KIAA0865 sequence did not reveal significant homology to any known myosin proteins. Taken together, these sequence data suggested that the KIAA0865 cDNA was most likely a partial cDNA clone that did not extend far enough 5′ to include the ATP binding site and the additional upstream N-terminal sequence identified in the myr 8a sequence and, accordingly, pointed to the possible existence of multiple myr 8 isoforms arising as a consequence of differential splicing of the C-terminal tail domain. Splice variants have been described previously for multiple mammalian unconventional myosins, including myosin I (Sherr et al., 1993), myosin V (Huang et al., 1998a,b; Lambert et al., 1998), myosin VIIA (Chen et al., 1996; Kelley et al., 1997; Mburu et al., 1997), myosin IXA and IXB (Chieregatti et al., 1998 Grewal et al., 1999), and class XV (Liang et al., 1999).

Identification and characterization of the myr 8b sequence

To identify a possible C-terminal splice variant of myr 8a, we performed PCR-based analyses with cDNAs prepared from postnatal day 10 rat cerebellar granule neurons using a sense primer common to both myr 8a and KIAA0865 and antisense primers that were unique either to the myr 8a 3′-untranslated sequence or to the KIAA0865 sequence (Fig. 2). PCR amplification performed with the antisense primer unique to the 3′-untranslated sequence of myr 8a generated a cDNA product with a sequence that was identical to myr 8a (clone 4), including the stop codon. PCR amplification using the antisense primer unique to the 3′ sequence of KIAA0865 yielded a product with a sequence that lacked the stop codon identified in myr 8a and thus continued further in the 3′ direction in the open reading frame (Fig. 2). This

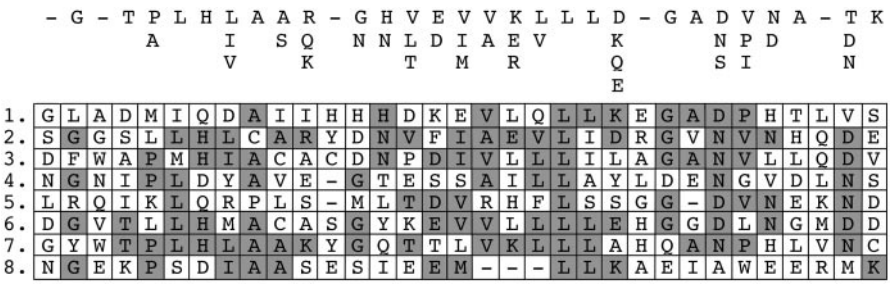

Figure 1. N-terminal extension of myr 8a shows eight ankyrin repeat sequences. Alignment of the myr 8a clone 4 sequence with the consensus sequence for ankyrin repeats reveals an array of eight ankyrin repeats in the N-terminal extension. Myr 8a amino acids that are identical to the ankyrin consensus sequence are indicated by *gray boxes*. Amino acid numbering for ankyrin repeats is as follows: *1*, G59-S91; *2*, S92-E124; *3*, D125-V157; *4*, N158-S189; *5*, L190-D220; *6*, D221-D253; *7*, G254-C286; *8*, N287-K316. The consensus sequence for ankyrin repeats is taken from Michaely and Bennett (1992).

extended C-terminal sequence obtained for rat was 71% identical at the amino acid level to that deduced from the human KIAA0865 cDNA. The variance in sequence likely reflects the difference in species.

To confirm the identity of the second myr 8 isoform, the PCR product generated from rat, which demonstrated high homology to the KIAA0865 sequence, was used as a cDNA probe (probe 4) to further screen the astrocyte cDNA library. The screen identified two clones: clone 8 composed of 2262 bp and clone 18 composed of 2849 bp. Sequence analyses indicated that clones 8 and 18 shared 100% identity to the PCR product used as a hybridization probe and 73% identity to the sequence of the KIAA0865 cDNA. Clone 18 lacked the stop codon translated in myr 8a/clone 4 and extended the sequence in open reading frame for an additional 590 amino acids. The nucleotide and deduced amino acid sequences of myr 8b cDNA C terminus, clone 18, are available from GenBank/EMBL/DDBJ (accession no. AY004215). The stop codon identified in clone 18 (nt 5776–5778) was followed by a 3′-untranslated region and a consensus polyadenylation sequence (AATAAA, nt 6825–6831) located 12 nucleotides upstream of the poly(A) tail, thereby indicating that the 3′ coding sequence was complete. Taken together, these sequence data are consistent with the interpretation of two myr 8 isoforms, which differ only in the length of the C-terminal tail domain. We have designated this second, larger myosin as myr 8b (eighth unconventional myosin from rat, isoform b). The extended C-terminal tail of myr 8b comprises ~750 amino acids, bears a net neutral charge, and reveals multiple stretches of poly-proline residues. Similar to the tail domain of myr 8a, the tail domain of myr 8b does not contain any predicted α-helical coiled-coil structures, suggesting that myr 8b also exists as a monomer. The open reading frames of myr 8a and 8b correlate to proteins with calculated molecular masses of ~148,748 and 210,557 Da, respectively.

The inferred relationships between rat cDNA clone 4 and clone 18 and human cDNA clone KIAA0865 and the corresponding proteins myr 8a, myr 8b, and KIAA0865, respectively, are shown in schematic form (Fig. 3*A*). Clone 4 contains a single open reading frame that codes for myr 8a in its entirety. Clone 18 overlaps clone 4 at the 3′ terminus, but because clone 18 lacks the stop codon identified in clone 4, the open reading frame is extended in the 3′ direction. Together, clone 4 and clone 18 comprise myr 8b. The homologous human cDNA clone KIAA0865 overlaps most of clone 4 and all of clone 18 and likely comprises the human ortholog to myr 8b.

The human cDNA clone KIAA0865 maps to chromosome 13 (UniGene Cluster: Hs.175411; LocusLink 23026). Comparative analysis of KIAA0865 genomic and cDNA sequences reveals an intron sequence that interrupts the KIAA0865 protein coding sequence as ANE-intron-ALAR (Fig. 3*B*). The consensus exon–intron splice junction (Mount, 1982) starts at nucleotide 2717997 (5′-AGgt. . . //. . . agCT-3′) and is identical to that position (nucleotide 4002, 5′-AG/CT-3′) where myr 8b and myr 8a sequences also diverge (Fig. 3*C*). Although we have not determined the genomic organization of myr 8, these data are consistent with the interpretation that the myr 8b sequence arises by intron removal, similar to that situation demonstrated for the KIAA0865 cDNA. In contrast, the myr 8a sequence is derived by crossing through the exon–intron splice junction. Accordingly, the myr 8a-specific sequence, which is a single amino acid (glycine 1322), comprises an exon in myr 8a but an intron in myr 8b (Fig. 3*D*).

Interestingly, the intervening intron in KIAA0865 (nt 2717999–2730710) does not include a stop codon in the same position as revealed for myr 8a but extends the coding sequence for an additional 16 amino acids (Fig. 3*E*). This human sequence, however, reveals a consensus polyadenylation sequence (AATAAA, nt 2718106–2718111) located within a ~30 nucleotide region that is well conserved with that sequence identified for rat myr 8a. Of multiple expressed sequence tags (ESTs) that match the KIAA0865 sequence, two, one from fetal liver and spleen (GenBank accession no. AA676319) and one from lung (GenBank accession no. AI690141), cross through the exon–intron splice boundary and continue for an additional 16 amino acids until reaching the in-frame stop codon. These EST sequence data are consistent with the expression in human of KIAA0865, which is similar to myr 8b, as well as a KIAA0865 isoform that is similar in length and structure to myr 8a.

Myr 8 proteins comprise a new class of unconventional myosins

The presence of unique structural features in both the head and tail domains suggested that myr 8 proteins might comprise a new class of myosins. To evaluate this possibility, the amino acid sequence of the myr 8a/8b head domain was aligned with representative members of all myosin classes, and a phylogenetic tree was constructed (Fig. 4). Analysis of this unrooted genetic distance tree indicates that myr 8 myosins are sufficiently divergent from known myosins as to comprise a new myosin class that, in keeping with previous numbering of myosin classes, we designated class XVI (Mermall et al., 1998; Probst et al., 1998; Wang et al., 1998). A recent phylogenetic analysis of the myosin superfamily by Hodge and Cope (2000) is in accordance with our designation of myr 8 myosins as a new class in the myosin superfamily.

Our analysis indicates that myr 8 myosins diverge from class IX myosins, which are characterized by a GTPase-activating protein domain and the zinc-binding C_6H_2 motif located within the C-terminal tail (Reinhard et al., 1995; Wirth et al., 1996; Müller et al., 1997; Chieregatti et al., 1998; Gorman et al., 1999; Grewal et al., 1999). Structurally, myr 8 myosins appear most closely related to the class III myosins (Montell and Rubin, 1988; Battelle et al., 1998), although the phylogenetic placement of *ninaC* ap-

```
                1251
Myr8a PCR:      ~~~~~~~~~~ ~~~~~~~~~~ ~~~~~~~~~~
Myr8a clone:    KRAEDQGGCR HAHSNSVPVP MAVDSLAQAL
Myr8b PCR:      ~~~~~~~~~~ ~~~~~~~~~~ ~~~~~~~~~~
KIAA0865:       KRTDDKSGPR HFHPSSMSVC AAVDGLGQCL

                1281
Myr8a PCR:      ~~~~~~~~~~ ~~~~~~~~~~ ~~~~~~~~~P
Myr8a clone:    AGPSSRSPSL HSVFSMDDST GLPSPRKQPP
Myr8b PCR:      ~~~~~~~~~~ ~~~~~~~~~~ ~~~~~~~~SP
KIAA0865:       VGPSIWSPSL HSVFSMDDSS SLPSPRKQPP

                1311
Myr8a PCR:      PKPKRDPNTR LSASYEAVSA CLSATKDAAS
Myr8a clone:    PKPKRDPNTR LSASYEAVSA CLSATKDAAS
Myr8b PCR:      PKPKRDPNTR LSASYEAVSA CLSATKDAAS
KIAA0865:       PKPKRDPNTR LSASYEAVSA CLSAAREAAN

                1341
Myr8a PCR:      EG*PREGQVN AVLTAHSWAG FW~~~~~~~~
Myr8a clone:    EG*PREGQVN AVLTAHSWAG FWSGSARGTI
Myr8b PCR:      EALTRPRPHS DDYSTMKKIP .PRKPKRSPH
KIAA0865:       EALARPRPHS DDYSTMKKIP .PRKPKRSPN

                1371
Myr8a PCR:      ~~~~~~~~~~ ~~~~~~~~~~ ~~~~~~~~~~
Myr8a clone:    VALI*LFFLI EINLIVGL~~ ~~~~~~~~~~
Myr8b PCR:      TKLSGSYEEI WGPRPSGTMG QVGKHHAPGT
KIAA0865:       TKLSGSYEEI SGSRP....G DARPAGAPG.

                1401
Myr8a PCR:      ~~~~~~~~~~ ~~~~~~~~~~ ~~~~~~~~~~
Myr8a clone:    ~~~~~~~~~~ ~~~~~~~~~~ ~~~~~~~~~~
Myr8b PCR:      LGVQWASPDS MPQCTPQLPL HLPLPQGDYD
KIAA0865:       .....AAARV LTPGTPQCAL PPAAPPGD.E

                1431
Myr8a PCR:      ~~~~~~~~~~ ~~~~~~~~~~ ~~~~~~~~~~
Myr8a clone:    ~~~~~~~~~~ ~~~~~~~~~~ ~~~~~~~~~~
Myr8b PCR:      DDGEPVYIEM VGNAARAGGS ETDSPDQGES
KIAA0865:       DDSEPVYIEM LGHAAR.... .PDSPDPGES

                1461
Myr8a PCR:      ~~~~~~~~~~ ~~~~~~~~~~ ~~~~~~~~~~
Myr8a clone:    ~~~~~~~~~~ ~~~~~~~~~~ ~~~~~~~~~~
Myr8b PCR:      VYEEMKYVLP EEGCGPGMLT FL..PASPPL
KIAA0865:       VYEEMKCCLP DDG.GPGAGS FLLHGASPPL

                1491
Myr8a PCR:      ~~~~~~~~~~ ~~~~~~~~~~ ~~~~~~~~~~
Myr8a clone:    ~~~~~~~~~~ ~~~~~~~~~~ ~~~~~~~~~~
Myr8b PCR:      FLETRKAIIL EAGEGSCQPL KDTCDIPPPF
KIAA0865:       LHRAPE.... ...DEAAGPP GDACDIPPPF

                1521
Myr8a PCR:      ~~~~~~~~~~ ~~~~~~~~~~ ~~~~~~~~~~
Myr8a clone:    ~~~~~~~~~~ ~~~~~~~~~~ ~~~~~~~~~~
Myr8b PCR:      PNLLPHRPPL LVFPPTPVTC SPA~~~~~~~
KIAA0865:       PNLLPHRPPL LVFPPTPVTC SPASDESPLT
```

Figure 2. Comparative alignment of the amino acid sequences deduced from PCR products amplified using sense primers common to both myr 8a (clone 4) and cDNA KIAA0865 and antisense primers unique to either 3′-untranslated sequence of myr 8a or KIAA0865. PCR amplifications were performed using cDNA prepared from granule neurons isolated from postnatal day 10 rat cerebellum. Sequence 1 was generated using a sense primer common to both myr 8a and KIAA0865 with an antisense primer unique to 3′-untranslated sequence of myr 8a. This product is identical to the 3′ terminus of myr 8a (clone 4) including the stop codon. Sequence 2 was generated using the sense primer common to both myr 8a and KIAA0865 with the antisense primer unique to the KIAA0865 sequence. This product does not encode a stop codon, therefore extending the sequence of myr 8a (clone 4) in the C-terminal direction. This extended sequence, which identifies the initial segment of the C-terminal tail domain of myr 8b, is 71% identical to the sequence described for the human cDNA KIAA0865. The sense and antisense primers correspond to the nucleotides of the amino acids indicated in *bold text*.

pears in <50% of our bootstrap data sets. Analogous to the structure of myr 8 myosins, *ninaC* reveals a similarly sized N-terminal extension, bears a positively charged C-terminal domain of two different lengths that contribute to two differentially expressed isoforms, and is predicted to function as a single-headed myosin (Porter et al., 1992). Interestingly, the N-terminal extension of *ninaC* and related class III myosins demonstrate serine/threonine protein kinase activity (Montell and Rubin, 1988; Ng et al., 1996; Battelle et al., 1998).

Myr 8b mRNA is the principal form expressed in neural and non-neural tissues

Northern blot analysis of poly(A) RNA prepared from type 1 astrocytes using probe 1 (nucleotides 1705–2220) revealed a single prominent hybridization signal of ~7.2 kb in size, a message size consistent with that anticipated for myr 8b (Fig. 5*A*). To confirm whether the ~7.2 kb message corresponded to myr 8b, we performed Northern blot analyses of poly(A) RNA and total RNA prepared from neocortex and cerebellum, respectively, at multiple developmental time points using probes that corresponded to the sequence common to both myr 8a and myr 8b (probe 1, nucleotides 1705–2220; probe 2, nucleotides 2788–3237; and probe 3, nucleotides 3436–3675), as well as with probes directed toward a sequence unique to the C-terminal tail domain of myr 8b (probe 4, nucleotides 3905–4600; and probe 5, nucleotides 4110–4771). These studies demonstrated for all probes a single, prominent signal of ~7.2 kb in apparent size in both neocortex and cerebellum (Fig. 5*B–D*). Because all probes common to both myr 8a and myr 8b as well as probes unique to myr 8b recognize a single, ~7.2 kb message, these data are in accordance with the interpretation that the ~7.2 kb message corresponds to myr 8b. Furthermore, these data imply that myr 8b comprises the predominant myr 8 isoform expressed in astroglial cells as well as in developing and adult brain. Although the signal at ~7.2 kb was detected at all developmental ages, the expression level detected both in neocortex and in cerebellum peaked during the first and second postnatal weeks, a time that coincides with ongoing neuronal cell migration and axonal process extension and dendritic elaboration. The message levels were significantly reduced in the adult. These data suggest the possibility that myr 8b mRNA expression, and potentially myr 8b protein, is regulated during brain development. The inability to detect myr 8a mRNA expression potentially reflects a minor role for myr 8a in cellular functions and/or the participation of myr 8a in a distinct aspect of brain development not examined in the present analysis.

To investigate the distribution of myr 8 mRNA expression, total RNA was prepared from multiple neural and non-neural tissues at postnatal day 10 and processed for Northern blot analysis using probe 2, which is directed to a sequence in common to both myr 8a and myr 8b, and with probe 4, which is directed toward a sequence unique to the C-terminal tail domain of myr 8b (Fig. 5*E*,*F*). For both probes, a prominent hybridization signal located at ~7.2 kb was observed in multiple regions of the CNS and to a lesser extent in adrenal and in cardiac and skeletal muscle. These data suggest that myr 8b is expressed predominantly in the nervous system. No signal was detected in other peripheral tissues. A weaker signal located at ~9.2 kb, which was restricted to regions of the CNS, was identified only for analyses performed using total RNA. We have not performed analyses to evaluate this additional message.

Myr 8b protein is the principal isoform expressed in neural and non-neural tissues

To investigate the distribution of myr 8b protein, polyclonal antibodies were raised against a peptide sequence specific to the C-terminal tail domain of myr 8b (amino acids 1763–1785) as well

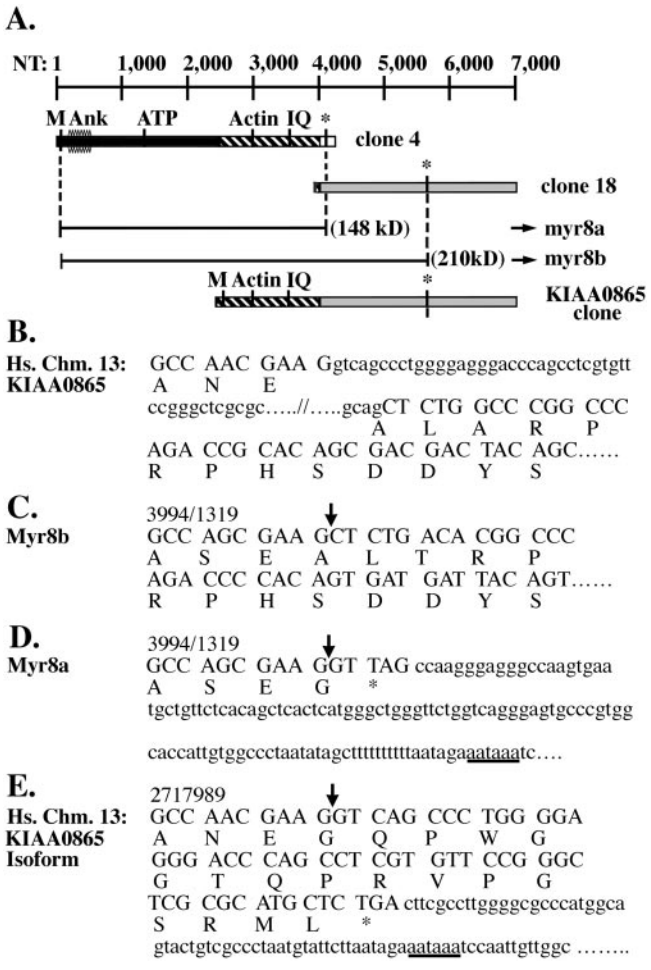

Figure 3. Relationships among myr 8a, myr 8b, and KIAA0865. Schematic diagram of inferred relationships between rat cDNA clone 4 and clone 18 and human cDNA clone KIAA0865 and the corresponding proteins myr 8a, myr 8b, and KIAA0865, respectively. Clone 4 contains a single open reading frame and codes for myr 8a. Clone 18 overlaps with the terminal 3′ sequence of clone 4 but lacks the stop codon identified in the clone 4 sequence and thus extends in the C-terminal direction. Together, clone 4 and clone 18 comprise myr 8b. The homologous human cDNA clone KIAA0865 overlaps most of clone 4 and all of clone 18. The overlapping region of identity for the rat myr 8 clone 4 and clone 18 and the human KIAA0865 sequences is indicated by the *hatched pattern*. At the 3′ terminus, the clone 4 (*white*) sequence diverges from clone 18 and KIAA0865 sequences (*gray*). The 5′ terminus of clone 4 (*black*) contains the ATP binding site and the ankyrin repeats (*A*). The human cDNA clone KIAA0865 maps to chromosome 13. Comparison of genomic and cDNA sequences reveals an intron sequence (*lowercase letters*) located between amino acids ANE and ALAR (*B*). The site where myr 8a and myr 8b sequences diverge corresponds to a consensus exon–intron boundary (indicated by *arrow*), starting at nucleotide 4002 and reading 5′-AG/GT-3′, that is identical to that demonstrated for KIAA0865. The myr 8b sequence, analogous to KIAA0865, is obtained by use of the splice junction (indicated by *arrow*) (*C*), whereas myr 8a is derived by crossing through the splice junction (indicated by *arrow*) (*D*). The intervening intron in KIAA0865 (starting at nt 2717999) does not include a stop codon in the same position as revealed for myr 8a but extends the coding sequence for an additional 16 amino acids. This human sequence, which contributes unique sequence to the KIAA0865 isoform, reveals a consensus polyadenylation sequence (AATAAA, nt 2718106–2718111) located within a ~30 nucleotide region that is well conserved with that sequence identified for rat myr 8a (*E*). *Actin*, Actin binding site; *Ank*, ankyrin repeats; *ATP*, ATP binding site; *IQ*, IQ motif domain; *M*, Kozak start sites; *asterisk* indicates stop codon. The scale bar represents nucleotide number. The predicted nucleotide length and molecular masses are noted for myr 8a and myr 8b. The deduced amino acid sequence is shown in *single-letter code* below the nucleotide sequence. The consensus polyadenylation signal (AATAAA) is *underlined*. *Lowercase* nucleotide sequence in *B* represents the intron sequence, whereas in *D* and *E*, the *lowercase* nucleotide sequence represents a 3′-untranslated sequence.

as to a recombinant fusion protein corresponding to amino acids 2–52 that comprises the N-terminal region located upstream of the ankyrin repeats domain in common with both myr 8a and 8b proteins. Antibodies were affinity purified and used for indirect immunofluorescence and immunoblot analyses. To identify the antigen(s) recognized by the developed antibodies, a cytoskeletal/membrane fraction was prepared from type 1 astrocytes and postnatal day 10 cerebellum, and polypeptides resolved by SDS-PAGE were processed for immunoblot analyses. Antibodies directed against either the N-terminal amino acids 2–52 (Fig. 6*A*) or the C-terminal tail domain of myr 8b (Fig. 6*B*) detected a single broad band that migrated with an apparent molecular mass of ~210 kDa. The apparent molecular mass of the detected antigen approximates that deduced from the primary sequence of myr 8b, i.e., 210,557 Da. Because antibodies directed to either the N terminus of myr 8b or to the C-terminal tail domain of myr 8b both recognize the identical antigen of ~210 kDa, these data demonstrate convincingly that the N-terminal ankyrin repeats domain contributes to the N-terminal extension of the myr 8b protein. On overexposed films, antibodies directed against the N-terminal amino acids 2–52, but not those antibodies directed toward the C-terminal domain of myr 8b, also detect minor bands having apparent molecular masses of ~145 kDa, which approximates that molecular mass deduced from the primary sequence of myr 8a, and ~170 kDa, an antigen that we have not characterized further (Fig. 6*C*).

To assess the tissue distribution of myr 8b protein, postnuclear supernatants were prepared for multiple brain regions as well as peripheral tissues, and proteins were processed for immunoblot analyses using antibodies directed against the N-terminal amino acids 2–52 (Fig. 7). A prominent ~210 kDa band was detected in all regions of the CNS, suggesting that myr 8b does not function in the CNS in a region-specific manner. In peripheral tissues, a prominent ~210 kDa band was detected in bladder (e.g., smooth muscle), lung, and kidney, and to a lesser degree in thymus, adrenal, and skeletal and cardiac muscles. Minor levels of immunoreactive bands corresponding to apparent molecular mass of ~170 and ~145 kDa were detected to varying extents among the different peripheral tissues. Last, Northern blot analyses and PCR amplifications performed using primers that corresponded to sequences located within the motor domain of myr 8b, as well as indirect immunolocalization using affinity-purified antibodies to the C-tail domain of myr 8b, indicated that NIH-3T3, CHO, RAT2, and COS-7 cells do not express myr 8a or myr 8b message or protein (data not shown).

Taken together, both immunoblot and Northern blot analyses indicate that myr 8b is the predominant myr 8 isoform expressed in brain, principally at developmental time periods, and in several peripheral tissues. The difference observed in myr 8b distribution as revealed by Northern blot analyses in comparison with immunoblot analyses likely reflects differences in the sensitivity of the two detection methods and, potentially, differences in the half-life of myr 8b mRNA versus myr 8b protein. Additional immunolocalization studies will be necessary to determine whether the detection of myr 8b in peripheral tissues is a consequence of associated neural tissue or because of the expression of myr 8b in non-neural cells.

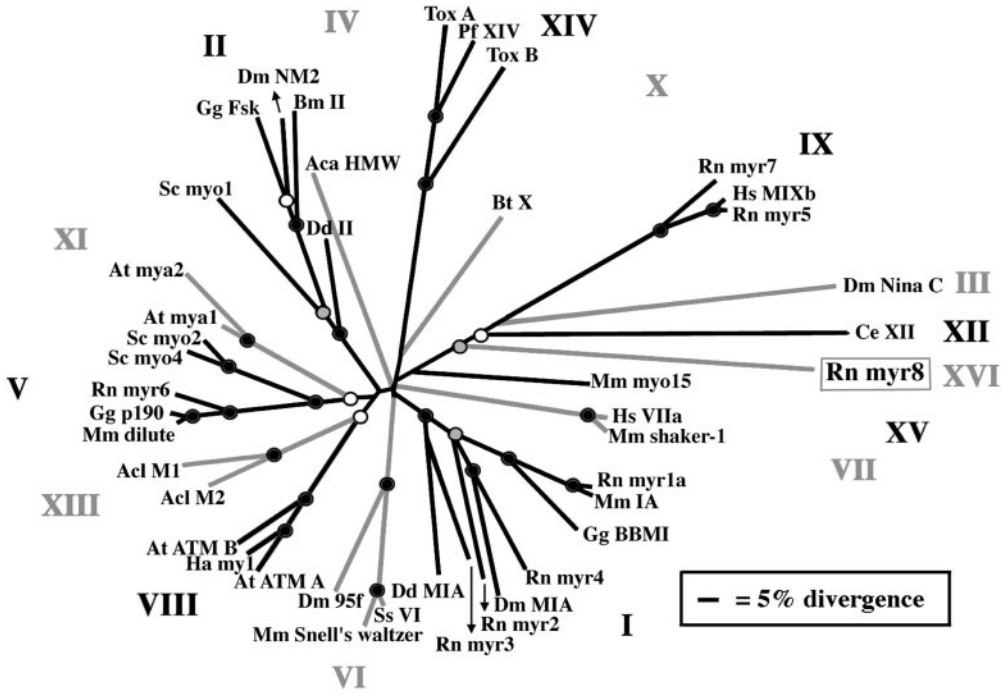

Figure 4. Unrooted phylogenetic tree of the myosin superfamily. Head domains of 40 myosin proteins available from public data bases were aligned to amino acids 213–511 of the chicken fast skeletal myosin (Gg FSK), a class II myosin, using the default CLUSTAL method settings (Lasergene/DNASTAR). The PHYLIP phylogeny package (http://evolution.genetics.washington.edu/phylip.html) (Felsenstein, 1993) was used to generate a genetic distance tree; 1000 bootstrap data sets were generated and analyzed with the programs PROTDIST and NEIGHBOR. The programs CONSENSE, FITCH, and DRAWTREE were used to produce the unrooted distance tree. The frequency of node placement for 1000 bootstrap trials is indicated as >90, >70, and >50% by *solid circles*, *gray circles*, and *open circles*, respectively. Sequence divergence is proportional to the length of the branches. The length of the bar equals 5% sequence divergence. Myosin classes are indicated by *Roman numerals*. The species represented are *Acanthamoeba castellanii* (*Aca*), *Acetabularia cliftonii* (*Acl*), *Arabidopsis thaliana* (*At*), *Brugia malayi* (*Bm*), *Bos taurus* (*Bt*), *Caenorhabditis elegans* (*Ce*), *Dictyostelium discoidium* (*Dd*), *Drosophila melanogaster* (*Dm*), *Gallus gallus* (*Gg*), *Helianthus annus* (*Ha*), *Homo sapiens* (*Hs*), *Mus musculus* (*Mm*), *Plasmodium falciparum* (*Pf*), *Rattus norvegicus* (*Rn*), *Saccharomyces cerevisiae* (*Sc*), *Sus scrofa* (*Ss*), and *Toxoplasma gondii* (*Tox*). The GenBank accession numbers for the sequences by class are as follows—class I: Dd MIA (P22467), Dm MIA (S45573), Gg BBMI (U04049), MmIA (L00923), Rn myr 1a (X68199), Rn myr 2 (X74800), Rn myr 3 (X74815), Rn myr 4 (X71997); class II: Bm II (M74000), Dd II (p08799), Dm NM2 (P05661), Gg Fsk (P13538), Sc myo1(IIA) (S46773); class III: Dm Nina C (p10676); class IV: Aca HMW (j05678); class V: Gg p190 (z11718), Mm dilute (x57377), Rn myr 6 (u60416), Sc myo2 (VA) (p19524), Sc myo4 (VB) (p32492); class VI: Dm 95F (Q01989), Mm Snell's waltzer (u49739), Ss VI (a54818); class VII: Hs VIIa (u55208), Mm shaker-1 (U81453); class VIII: At ATM A (x67104), At ATM B (z34292), Ha my1 (U94781); class IX: Hs MIXb (u42391), Rn myr 5 (x77609), Rn myr 7 (AJ001713); class X: Bt X (U55042); class XI: At mya1 (z29389), At mya2 (z34294); class XII: Ce XII (z66563); class XIII: Acl M1 (U94397), Acl M2 (U94398); class XIV: Tox A (af006626), Tox B (af006627), Pf XIV (y09693); class XV: Mm myo15 (AF053130); class XVI: Rn myr 8 (AF209114).

Myr 8b associates with the protein phosphatase catalytic subunits 1α and 1γ_1

Analysis of the myr 8b sequence reveals a four-residue consensus motif (KVRF, consensus R/K-V/I-X-F) identified in many protein phosphatase catalytic subunit binding proteins (Egloff et al., 1997; Hirano et al., 1997; Johnson et al., 1997). This motif is immediately followed by a series of eight ankyrin repeats that bears ~30% homology to a series of eight ankyrin repeats located at the N terminus (amino acids 1–295) of the large targeting subunit of myosin phosphatase. The large targeting subunit of myosin phosphatase binds to protein phosphatase 1 catalytic subunits through the N-terminal ankyrin repeats domain and myosin through interactions with its C-terminal domain (Hartshorne, 1998). To test the possibility that the myr 8 protein might participate in the selective targeting of a PP1 catalytic subunit, nonionic detergent extracts prepared from postnatal day 10 cerebellum were incubated with affinity-purified antibodies directed toward the C-terminal tail domain of myr 8b, and immunoisolated fractions were analyzed by immunoblotting for PP1 catalytic isoforms. As a first step, we performed immunoblots using a polyclonal antibody directed against multiple (1α, 1β, 1γ, 2A, 2B, and X) PP1 catalytic subunits (Fig. 8, *lane 1*). The pan PP1 catalytic subunit antibody recognized a single band that migrated with an apparent molecular mass between 35 and 40 kDa. To refine the identity of the precipitated protein phosphatase catalytic subunit, we next performed immunoblot analyses using polyclonal antibodies that were directed to selective PP1 catalytic subunits (Fig. 8, *lanes 2*, *3*, *4*, *5*). These results revealed that the catalytic subunits PP1α and PP1γ, but not PP1β, PP2a, or PP2b, coprecipitated with myr 8b protein. Previous studies have shown that the catalytic subunits PP1α and PP1γ localize to and associate with the actin cytoskeleton, whereas the catalytic subunit PP1β localizes to and associates with the microtubular cytoskeleton (Ouimet et al., 1995; Allen et al., 1997; Andreassen et al., 1998; MacMillan et al., 1999; McAvoy et al., 1999; Strack et al., 1999). Further immunoblot analysis revealed that actin also coprecipitated with myr 8b (Fig. 8, *lane 6*).

Analyses performed for other protein phosphatase catalytic subunit binding proteins demonstrate clearly that bound catalytic subunits are inactive (Hubbard and Cohen, 1989; Beullens et al., 1999; McAvoy et al., 1999). Although we have not determined whether the interaction between protein phosphatase catalytic subunits PP1α and PP1γ and myr 8b is regulated by phosphorylation, as demonstrated for other protein phosphatase catalytic subunit binding proteins (Hubbard and Cohen, 1989; Beullens et al., 1999; McAvoy et al., 1999; Toth et al., 2000), myr 8b contains a potential PKC phosphorylation site located at amino acid 53 (SQK), two amino acids upstream of the consensus protein phosphatase binding motif. This site correlates with the phosphorylation site located at amino acid 34 (threonine) of the large targeting subunit of myosin phosphatase (Hartshorne, 1998), for which

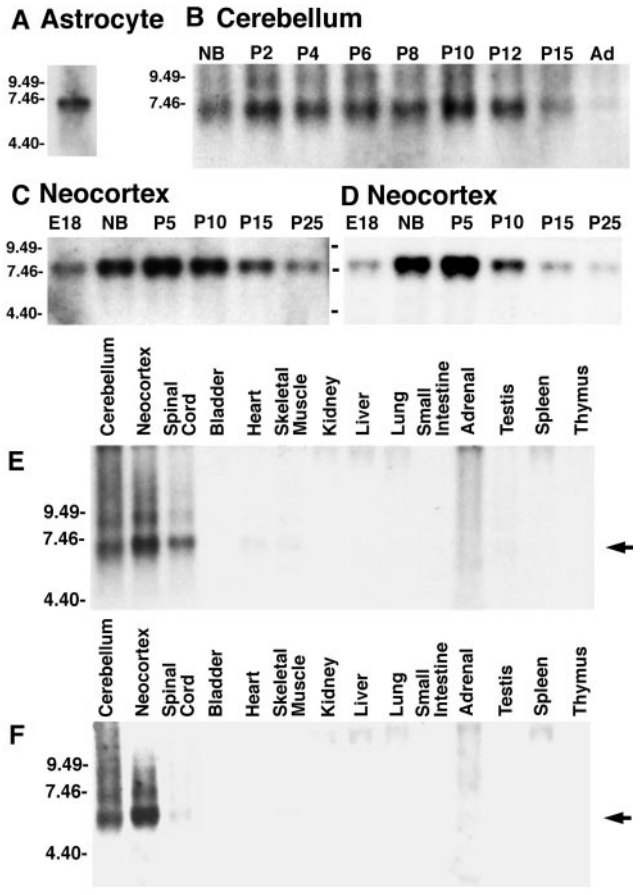

Figure 5. Tissue-specific expression of myr 8 mRNA. Northern blots of poly(A) RNA (2.5 μg/lane) from type 1 astrocytes (*A*), total RNA (15 μg/lane) from cerebella at indicated developmental time points (*B*), poly(A) RNA (2.5 μg/lane) from neocortices at indicated developmental ages (*C*, *D*), and total RNA (15 μg/lane) from the indicated tissues obtained at postnatal day 10 (*E*, *F*) were hybridized with ^{32}P-labeled probe 1 (*A*, *B*), probe 2 (*C*, *E*), probe 4 (*F*), and probe 5 (*D*). A prominent signal of ~7.2 kb was detected in astrocytes and at all developmental ages for both neocortex and cerebellum, although the level of the ~7.2 kb message peaked during the first and second postnatal weeks in both neocortex and cerebellum. The ~7.2 kb myr 8 transcript (*arrow*) was detected principally in the CNS but was also observed to a minimal extent in adrenal and heart and skeletal muscle. Equal RNA loads were verified by evaluation of 18S ribosomal RNA after ethidium bromide staining. RNA size standards are indicated in kilobases. *Ad*, Adult; *E*, embryonic day; *NB*, newborn; *P*, postnatal day.

PKC phosphorylation induces dissociation of the catalytic subunit (Toth et al., 2000).

Myr 8b cosediments with F-actin in an ATP-sensitive manner

To determine whether myr 8b bound actin in an ATP-sensitive manner, a characteristic feature of myosin motor proteins, we performed F-actin cosedimentation assays as described by Cheney and colleagues (Berg et al., 2000). Aliquots of a detergent-soluble lysate were prepared from postnatal day 8 brain, and the association of soluble myr 8b with platelet actin in the presence and absence of ATP was assessed by immunoblot analysis using antibodies directed against the N-terminal amino acids 2–52. In the presence of either 0.5 or 1 mM ATP, myr 8b did not cosediment with F-actin to a significant level. In contrast, after depletion of ATP by inclusion of hexokinase, a significant portion of soluble myr 8b cosedimented with F-actin (Fig. 9).

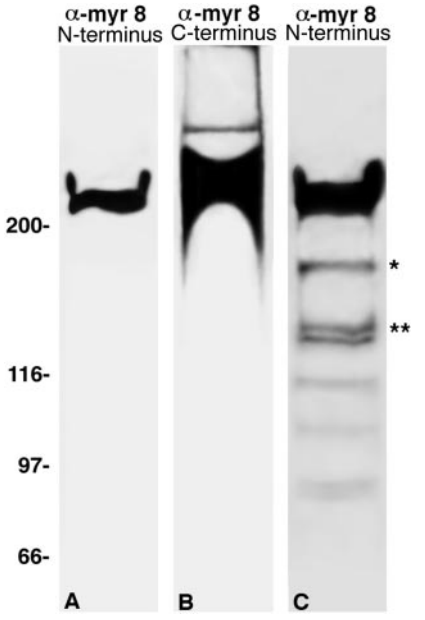

Figure 6. Antibodies directed against either N-terminal amino acids 2–52 or C-terminal amino acids 1763–1785 recognize principally a ~210 kDa antigen. A cytoskeletal/membrane fraction was isolated from postnatal day 10 brain (*A*, *C*) and from neocortical type 1 astrocytes (*B*). Polypeptides were resolved by SDS-PAGE and processed for immunoblot analyses using antibodies directed toward the N-terminal amino acids 2–52 (*A*, *C*) or affinity-purified antibodies directed toward the C-terminal amino acids 1763–1785 located within the tail domain of myr 8b (*B*). Both antibodies detect a single broad immunoreactive band migrating with an apparent molecular mass of ~210 kDa. Overexposure of immunoblots performed using the antibody directed against the N-terminal amino acids 2–52 reveals two minor band of ~148 kDa (**) and ~170 kDa (*).

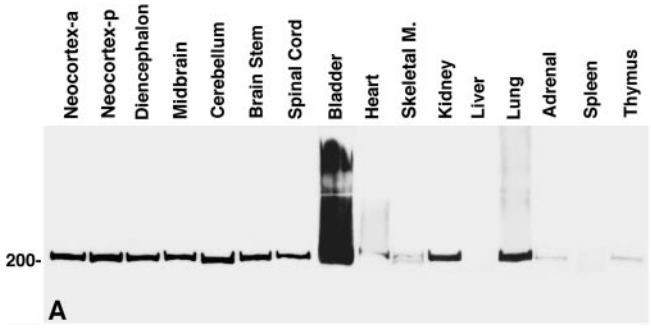

Figure 7. Tissue distribution of myr 8 protein. Post-nuclear supernatants were prepared from the indicated tissues obtained at postnatal day 10, and proteins were resolved by SDS-PAGE and processed for immunoblot analysis using antibodies directed toward the N-terminal amino acids 2–52. A broad immunoreactive band migrating with an apparent molecular mass of ~210 kDa was the principal antigen detected in both neural and non-neural tissues. *a*, Anterior; *p*, posterior. Molecular mass $\times 10^{-3}$ is indicated *vertically*.

These data demonstrate that myr 8b myosin can bind to actin, either directly or indirectly, in an ATP-sensitive manner.

Myr 8b in brain exists in both soluble and sedimentable subcellular pools

To begin to investigate the subcellular distribution of myr 8b, homogenates prepared from postnatal day 8 brain tissue in the presence and absence of ATP were subfractionated by differential velocity sedimentation, and proteins for each isolated fraction were processed for quantitative immunoblot analysis using anti-

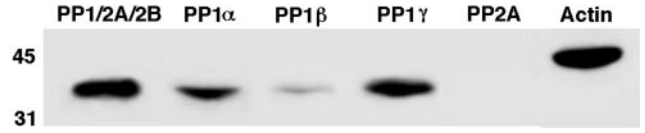

Figure 8. Myr 8b associates with the protein phosphatase catalytic subunits 1α and 1γ1. A crude cytoskeletal/membrane fraction prepared from postnatal day 10 cerebellum was solubilized in 1% Triton X-100, and unsolubilized components were sedimented by centrifugation. Aliquots of the detergent lysate were processed for immunoprecipitation using affinity-purified antibodies directed toward the C-terminal tail domain of myr 8b. Immunoprecipitated polypeptides were resolved by SDS-PAGE and processed for immunoblot analyses using polyclonal antiserum directed against multiple (1α, 1β, 1γ, 2A, 2B, and X) and individual (*PP1*α), (*PP1*β), (*PP1*γ), and (*PP2A*) protein phosphatase catalytic subunits and actin. Molecular mass $\times 10^{-3}$ is indicated *vertically*.

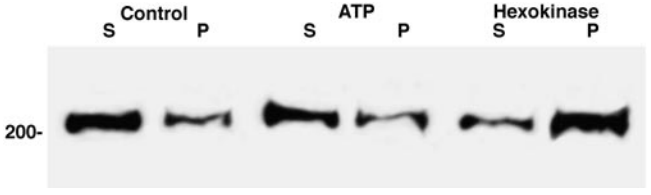

Figure 9. Myr 8b cosediments with F-actin in an ATP-sensitive manner. Postnatal day 8 brain was homogenized in the presence of 0.5 mM ATP, and a soluble fraction was obtained by high-speed centrifugation. Supernatant samples (100 μg protein) were supplemented with glucose (50 mM) and 50 μg platelet nonmuscle actin (*Control*); glucose, platelet nonmuscle actin, and 1 mM ATP (*ATP*); and glucose, platelet nonmuscle actin, and 0.5 U hexokinase (*Hexokinase*). After incubation (15 min at 25°C), centrifugation yielded a supernatant (*S*) and a pellet (*P*), which were collected, resolved by SDS-PAGE, and processed for immunoblot analysis using antibodies directed toward the N-terminal amino acids 2–52. Molecular mass $\times 10^{-3}$ is indicated *vertically*.

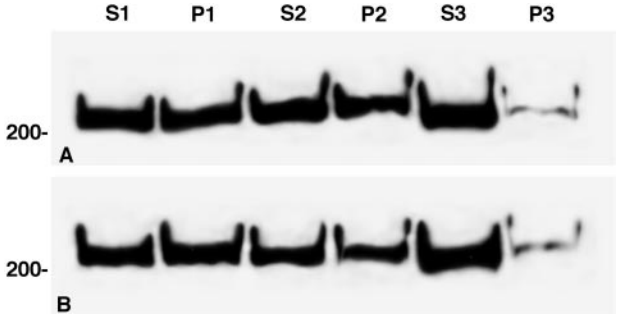

Figure 10. Myr 8b in brain exists in both soluble and sedimentable subcellular pools. Postnatal day 8 brain was homogenized in the absence (*A*) and presence (*B*) of 0.5 mM ATP and fractionated by velocity sedimentation. Equal protein loads were resolved by SDS-PAGE and processed for immunoblot analysis using antibodies directed toward the N-terminal amino acids 2–52. *S1*, *P1*: 1000 $\times$ *g* $\times$ 10 min supernatant (*S*) and pellet (*P*); *S2*, *P2*: 10,000 $\times$ *g* $\times$ 15 min supernatant (*S*) and pellet (*P*); *S3*, *P3*: 100,000 $\times$ *g* $\times$ 60 min supernatant and pellet.

bodies directed against the N-terminal amino acids 2–52 (Fig. 10). In the absence of ATP (Fig. 10*A*), ~60% of myr 8b immunoreactivity remained in the 1000 $\times$ *g* supernatant (S1). Of this soluble myr 8b immunoreactivity, ~85% distributed to the 100,000 $\times$ *g* supernatant (S3). In the presence of ATP (Fig. 10*B*), ~80% of myr 8b immunoreactivity distributed to the 1000 $\times$ *g* supernatant (S1), and of this soluble myr 8b immunoreactivity, ~85% was recovered in the 100,000 $\times$ *g* supernatant fraction (S3). Relative to the homogenate, myr 8b immunoreactivity normalized to protein is enriched approximately two times in the 100,000 $\times$ *g* supernatant fraction (S3). These data indicate that myr 8b distributes to two pools, a membrane-associated pool and a soluble cytoplasmic pool. Ongoing studies are directed toward determining the means of modulating the distribution between the two pools and whether the two pools reflect distinct states of myr 8b association with protein phosphatase catalytic subunits.

Myr 8b protein localizes in a punctate manner in primary astroglial and neuronal cells

To investigate the cellular and subcellular distribution of myr 8b protein, we performed indirect immunofluorescent analyses using aldehyde-fixed primary cell cultures of type 1 astrocytes, cerebellar granule neurons, hippocampal neurons, and preparations containing migrating cerebellar granule neurons.

In type-1 astrocytes, myr 8b immunoreactivity was observed typically as individual, intensely fluorescent puncta located throughout the region of the cell body as well as along the length of extended processes (Fig. 11*A*). On occasion, myr 8b immunoreactivity was organized in linear arrays or large clusters that localized about the nucleus (Fig. 11*B*).

In primary cell cultures of cerebellar granule neurons and hippocampal neurons, a prominent level of immunoreactivity was displayed throughout the somal cytoplasm (Fig. 11*C*,*D*,*G*), as well as along the entire length of all neurite processes (Fig. 11*D*,*G*). In many neurons, immunoreactivity appeared to distribute to the underlying surface of the plasma membrane (Fig. 11*E*). In cell dissociates of postnatal day 8 cerebellum, cells having the morphological features characteristic of migrating granule neurons revealed fluorescent puncta throughout the cell body and along the length of the leading process (Fig. 11*F*).

Myr 8b localizes to migrating granule neurons in developing cerebellum

To determine whether the pattern of myr 8b expression correlated to a unique event during brain development, we performed indirect immunofluorescent analyses using frozen sections of cerebellum prepared at postnatal day 10 and adult. At postnatal day 10, descension of granule neurons from the external granule cell layer is a prominent ongoing process. Purkinje cells are arranged as a monolayer, and processes of radial glial cells extend through the external granule cell layer to the pial surface (Altman and Bayer, 1997). Myr 8b immunoreactivity was localized preferentially to granule neurons located in the external granule cell layer, often to those located in the inner portion of the external granule cell layer (Fig. 12*A*). Within this location, granule neurons are in the initial stages of the migration process, extending membrane processes (a leading process and two trailing processes destined to become parallel fibers) and initiating translocation through the incipient molecular layer (Kuhar et al., 1993). A lesser degree of immunoreactivity was detected within the soma and dendrites of Purkinje cells. In the adult cerebellum, myr 8b immunoreactivity appeared reduced in intensity and was detected principally in Purkinje cell bodies and associated dendritic processes, in the elongated processes of radial glial cells, and in astrocytes and about the cell bodies of granule neurons located in the internal granule cell layer (Fig. 12*B*).

DISCUSSION

Myr 8 defines a novel mammalian myosin

We report the finding and initial characterization of myr 8a and myr 8b, which comprise the founding members of a novel class of

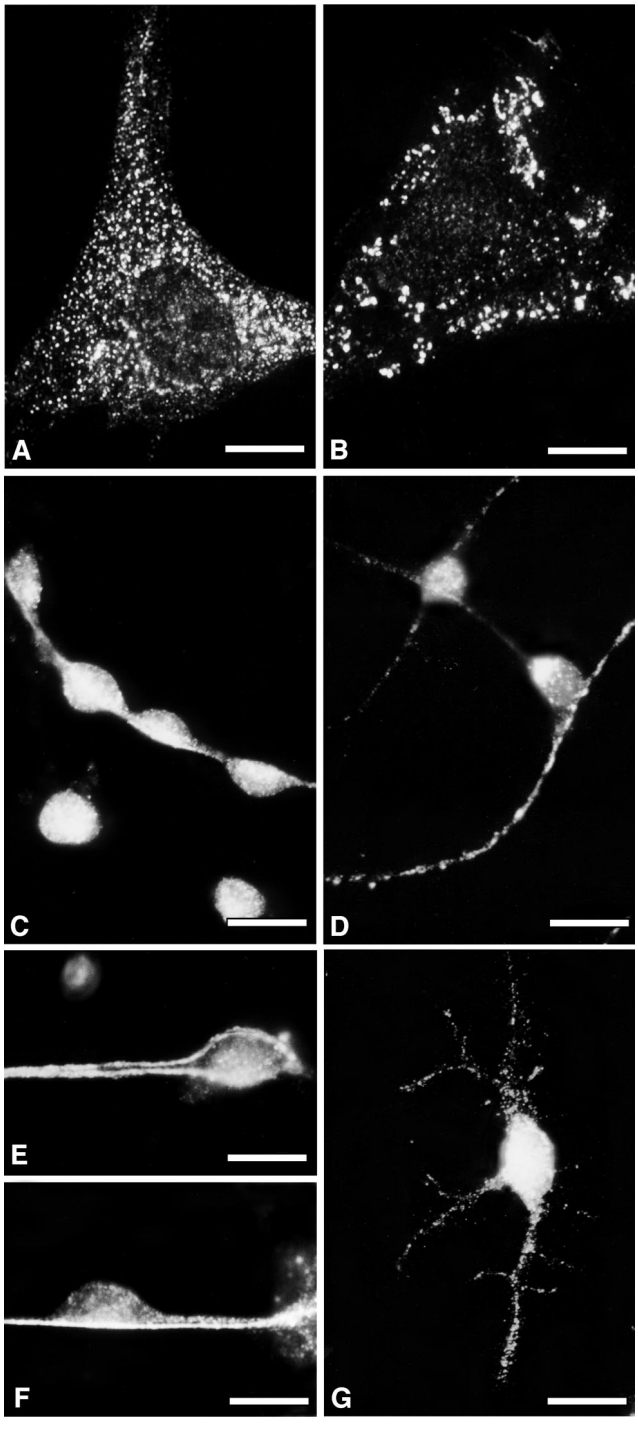

Figure 11. Immunofluorescent staining of myr 8b in primary cultures of astrocytes and neurons using affinity-purified antibodies directed toward the C-terminal tail domain of myr 8b. In neocortical and cerebellar type 1 astrocytes, myr 8b immunoreactivity was detected as intensely fluorescent puncta throughout the somal region and along the length of extended processes (*A*). Occasionally, immunoreactivity was organized in linear arrays or in large clusters located in a perinuclear position (*B*). In primary cultures of cerebellar granule neurons (*C–E*) and hippocampal neurons (*G*), myr 8b immunoreactivity was detected at a significant level in the cell body, but intense fluorescent puncta were also observed scattered along the entire length of both dendritic and axonal processes. In cell dissociates of neonatal cerebellum, granule neurons having the morphological features characteristic of migrating neurons displayed myr 8b immunoreactivity in a punctate manner throughout the cell body as well as along the length of the leading process (*F*). Scale bars: *A*, 10 μm; *B*, 10 μm; *C*, 18 μm; *D*, 15 μm; *E*, 10 μm; *F*, 10 μm; *G*, 18 μm.

myosins expressed at prominent levels in the developing nervous system. Examination of the myr 8 sequence reveals multiple motifs characteristic of myosins, in addition to an extended N terminus, that although unusual for myosins, is not without precedence (e.g., class III myosins). The N-terminal extension of myr 8 myosins reveals three in-frame consensus vertebrate translation initiation sequences (Kozak, 1991) located upstream of the consensus ATP binding site: methionine 1 (nt 40–42), methionine 251 (nt 790–792), and methionine 385 (nt 1192–1194). Alignment of the N terminus of myr 8 myosins to other myosins of multiple classes, and comparison of the length and relative position for each initiation sequence to the ATP binding consensus sequence (GERGSGKT) suggests that any of the methionines could serve as a potential start site: methionine 385 is characteristic of the position of the start site for myosins of class I, methionine 251 is comparable in location to the start site identified for myosins of class IX, and methionine 1 is similar in context to myosins of class III. Immunoblot analyses using antibodies directed to either the N terminus or the C-terminal of myr 8b reveal a single antigen of ~210 kDa (myr 8b), suggesting that methionine 1 serves as the principal translational start site for myr 8 myosins. Nonetheless, these data do not rule out the possible presence of additional myr 8 isoforms arising from potentially different start sites.

Myr 8b is the principal isoform expressed in neural and non-neural cells

Northern blot analyses of poly(A) RNA performed using probes common to myr 8a and myr 8b as well as unique to myr 8b consistently detect a single, prominent transcript of ~7.2 kb in size, a message size corresponding to the size anticipated for the myr 8b isoform. Likewise, immunoblot analyses demonstrate principally a single antigen with an apparent molecular mass approximating that deduced from the myr 8b amino acid sequence. Both of these data are consistent with the interpretation that myr 8b comprises the principal isoform expressed in neural and non-neural cells and with the possibility that myr 8a might exist only as a formal consideration. However, the presence of a consensus exon–intron splice junction at the point where the myr 8a and myr 8b sequences diverge, coupled with the identification of a putative polyadenylation signal (AATAA) that is located in an appropriate context to the poly(A) tail, implies that the myr 8a sequence does not represent an incompletely processed mRNA or a cloning artifact. Analysis of the myr 8a and 8b sequence reveals a consensus exon–intron splice junction precisely at the position where myr 8a and myr 8b sequences diverge. Importantly, analysis of the genomic sequence reveals that the human KIAA0865 sequence also contains an exon–intron boundary at precisely the identical position. PCR analyses performed using mRNA prepared from type 1 astrocytes, cerebellar granule neurons, and postnatal day 8 cerebellum with myr 8a 3′-untranslated sequence as the reverse primer (myr 8a has a unique 3′-untranslated sequence) identified selectively the myr 8a sequence, including the stop codon. These PCR data provide corroborative evidence in support of myr 8a expression. Furthermore, of multiple human ESTs that match the KIAA0865 sequence, two (GenBank accession no. AA676319 and AI690141) are consistent with the expression in human of a KIAA0865 isoform similar in structure to the myr 8a sequence. Accordingly, multiple sets of data are consistent with the likelihood of myr 8a myosin expression, although at a lower level in comparison with myr 8b myosin.

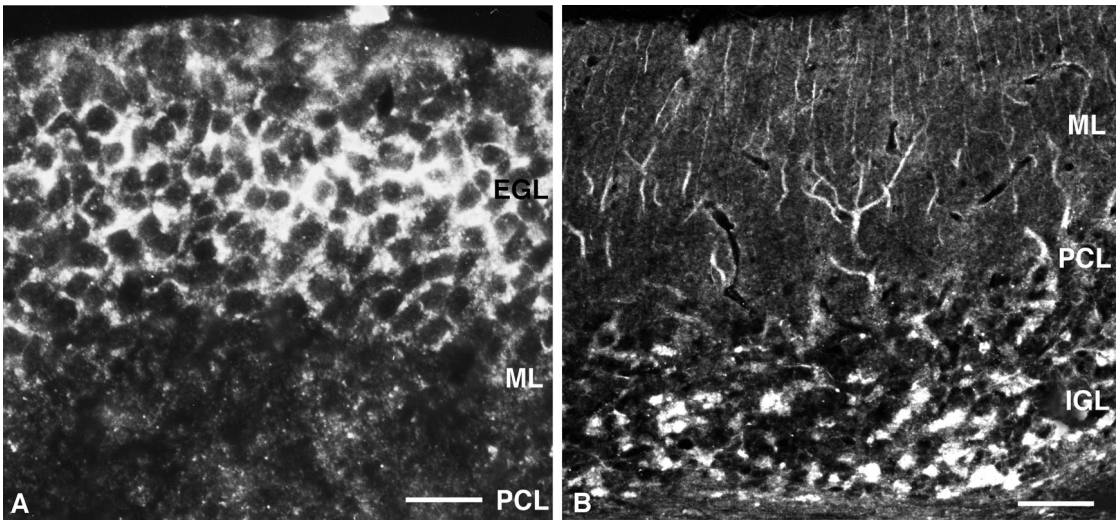

Figure 12. Immunolocalization of myr 8b in developing and adult cerebellum using affinity-purified antibodies directed toward the C-terminal tail domain of myr 8b. Frozen, 6 μm-thick sagittal sections were used. At postnatal day 10, myr 8b immunoreactivity was detected principally around granule neurons located in the inner portion of the external granule layer. A lesser degree of immunoreactivity was detected within the soma and dendrites of Purkinje cells (*A*). In the adult cerebellum, myr 8b immunoreactivity continued to be detected in Purkinje cell bodies and associated dendritic processes, in the elongated processes of radial glial cells, and in astroglial cells and cell bodies of granule neurons located in the internal granule cell layer (*B*). *EGL*, External granule cell layer, *IGL*, internal granule cell layer; *ML*, molecular layer; *PCL*, Purkinje cell layer. Scale bars: *A*, 14 μm; *B*, 45 μm.

Myr 8 may serve to target protein phosphatase catalytic subunits to select actin pools

The head domain of myr 8a/myr 8b reveals a four-residue consensus motif (KVRF) that corresponds to the consensus protein phosphatase 1 catalytic subunit binding sequence (R/K-V/I-X-F) identified in many protein phosphatase catalytic subunit binding proteins (Egloff et al., 1997; Hirano et al., 1997; Johnson et al., 1997). This motif is immediately followed by a series of eight ankyrin repeats that bears ~30% homology to a series of eight ankyrin repeats that mediate the interaction of protein phosphatase 1 catalytic subunits to the large targeting subunit of myosin phosphatase (Chen et al., 1994; Shimizu et al., 1994; Fujioka et al., 1998; Hartshorne, 1998). In accordance with the indicated sequence homology, the protein phosphatase catalytic subunits PP1α and PP1γ, but not PP1β or PP2a or 2b, coimmunoprecipitate using affinity-purified antibodies to the C-terminal tail domain of myr 8b.

The C-terminal tails of myr 8a and myr 8b are not predicted to display extensive α-helical coiled-coil structure. Thus, myr 8 isoforms likely function as single-headed myosins. Presently, the identified sequence variation between myr 8 isoforms appears to be restricted to the C terminus, which is that domain of myosins considered to dictate specific intracellular interactions and/or subcellular localization (Porter et al., 1992; Catlett and Weisman, 1998; Reck-Peterson et al., 1999; Schott et al., 1999; Tsakraklides et al., 1999). Consequently, the potential identification of differential splice variant tail domains raises the possibility of selective cellular and subcellular localizations and functions for individual myr 8 isoforms. The tail domain of myr 8a, which is relatively short and bears a net positive charge (pI of 9.6), resembles the C-terminal tails of class I myosins. Accordingly, myr 8a may bind to anionic macromolecules as has been demonstrated for class 1 myosins binding to anionic phospholipids (Adams and Pollard, 1989; Hayden et al., 1990). The extended tail domain of myr 8b has an overall neutral charge (pI of 6.9) and several short domains enriched in poly-proline residues. The poly-proline domain comprising amino acids 1588–1596 conforms to the 8–10 poly-proline consensus binding site sequence for profilin (Schluter et al., 1997), whereas the amino acid sequence F-P-P-T-P (amino acids 1510–1514) adheres loosely to the consensus binding site sequence F-P-P-P-P for the Ena/VASP protein family (Prehoda et al., 1999). These potential binding sites suggest that myr 8b may interact with several regulators of actin polymerization (Ayscough, 1998; Suetsugu et al., 1998; Machesky and Insall, 1999).

Myr 8 comprises a member of an expanding subset of myosin proteins that couple regulatory cell signaling functions to interactions with the actin cytoskeleton

In recent years, considerable data have revealed that components that participate in cell signaling events are assembled at restricted subcellular locations by clustering or through the interaction with anchoring, adaptor, or scaffolding proteins (Pawson and Scott, 1997; Kennedy, 2000). Among the serine/threonine phosphatases in brain, the catalytic subunits of protein phosphatase 1 have been shown to be associated with a number of targeting subunits (for review, see Price and Mumby, 1999), including neurabin I, a brain-specific F-actin binding protein implicated in the targeting of protein phosphatase 1α to growth cones (Nakanishi et al., 1997; McAvoy et al., 1999), and spinophilin (also known as neurabin II), a widely distributed F-actin binding protein implicated in the targeting of protein phosphatase 1α and 1γ to dendritic spines (Allen et al., 1997). Present immunolocalization studies reveal that myr 8b localizes in a punctate manner throughout the cell body and extended membrane processes of both neuronal and astroglial cells. The size and distribution of immunolabel is consistent with the possible association of myr 8b with intracellular transport vesicles. Considerable evidence implicates the actin cytoskeleton in regulating the dynamics of the Golgi complex, and recent data demonstrate actin as a component of Golgi membranes and Golgi-derived transport vesicles (Fucini et al., 2000; Valderrama et al., 2000). Likewise, myosin motor proteins have been shown to play a major role in vesicular transport and organelle retention (for review, see DePina and Langford, 1999; Sokac and Bement, 2000). In developing cerebellum, myr

8b immunoreactivity is localized principally to the inner portion of the external granule layer, a layer where granule cells begin to elaborate membrane processes as they initiate the process of migration. Importantly, considerable evidence implicates deficiencies in the regulation of both actin and microtubule dynamics in neuronal migration disorders (Gleeson and Walsh, 2000; Reiner, 2000).

In summary, myr 8a and myr 8b, the first members of Class XVI myosins, taken together with class III (Montell and Rubin, 1988), class V (Costa et al., 1999), and class IX (Reinhard et al., 1995; Wirth et al., 1996; Müller et al., 1997; Chieregatti et al., 1998) myosins, contributes to an expanding subset of myosin proteins that appear to couple regulatory cell signaling functions to interactions with the actin cytoskeleton (Bähler, 2000). We anticipate that future studies directed toward modulating endogenous levels of myr 8b will clarify the role of myr 8b in brain development.

REFERENCES

Adams RJ, Pollard TD (1989) Binding of myosin I to membrane lipids. Nature 340:565–568.

Allen PB, Ouimet CC, Greengard P (1997) Spinophilin, a novel protein phosphatase 1 binding protein localized to dendritic spines. Proc Natl Acad Sci USA 94:9956–9961.

Altman J, Bayer SA (1997) Development of the cerebellar system: in relation to its evolution, structure and function. Boca Raton, FL: CRC.

Altschul SF, Madden TL, Schaffer AA, Zhang J, Zhang Z, Miller W, Lipman DJ (1997) Gapped BLAST and PSI-BLAST: a new generation of protein database search programs. Nucleic Acid Res 25:3389–3402.

Andersen SSL, Bi GQ (2000) Axon formation: a molecular model for generation of neuronal polarity. BioEssays 22:172–179.

Andreassen PR, Lacroix FB, Villa-Moruzzi E, Margolis RL (1998) Differential subcellular localization of protein phosphatase-1α, γ1, and δ isoforms during both interphase and mitosis in mammalian cells. J Cell Biol 141:1207–1215.

Avraham KB, Hasson T, Steel KP, Kingsley DM, Russell LB, Mooseker MS, Copeland NG, Jenkins NA (1995) The mouse Snell's waltzer deafness gene encodes an unconventional myosin required for structural integrity of inner hair cells. Nat Genet 11:369–374.

Ayscough KR (1998) In vivo functions of actin-binding proteins. Curr Opin Cell Biol 10:102–111.

Bähler M (2000) Are class III and class IX myosins motorized signalling molecules? Biochim Biophys Acta 1496:52–59.

Bähler M, Kroschewski R, Stöffler H-E, Behrmann T (1994) Rat myr 4 defines a novel subclass of myosin I: identification, distribution, localization, and mapping of calmodulin-binding sites with differential calcium sensitivity. J Cell Biol 126:375–389.

Battelle B-A, Andrews AW, Calman BG, Sellers JR, Greenberg RM, Smith WC (1998) A myosin III from Limulus eyes is a clock-regulated phosphoprotein. J Neurosci 18:4548–4559.

Bement WM, Mooseker MS (1995) TEDS rule: a molecular rationale for differential regulation of myosins by phosphorylation of the heavy chain head. Cell Motil Cytoskeleton 31:87–92.

Bement WM, Hasson T, Wirth JA, Cheney RE, Mooseker MS (1994a) Identification and overlapping expression of multiple unconventional myosin genes in vertebrate cell types. Proc Natl Acad Sci USA 91:6549–6553.

Bement WM, Hasson T, Wirth JA, Cheney RE, Mooseker MS (1994b) Correction: Identification and overlapping expression of multiple unconventional myosin genes in vertebrate cell types. Proc Natl Acad Sci USA 91:11767.

Berg JS, Derfler BH, Pennisis CM, Corey DP, Cheney RE (2000) Myosin-X, a novel myosin with pleckstrin homology domains, associates with regions of dynamic actin. J Cell Sci 113:3439–3451.

Beullens M, Van Eynde A, Vulsteke V, Connor J, Shenolikar S, Stalmans W, Bollen W (1999) Molecular determinants of nuclear protein phophatase-1 regulation by NIPP-1. J Biol Chem 274:14053–14061.

Cameron PL, Sudhof TC, Jahn R, DeCamilli P (1991) Co-localization of synaptophysin with transferrin receptors: implications for synaptic vesicle biogenesis. J Cell Biol 115:151–164.

Cameron RS, Rakic P (1994) Identification of membrane proteins that comprise the plasmalemmal junction between migrating neurons and radial glial cells. J Neurosci 14:3139–3155.

Cameron RS, Ruffin JW, Cho NK, Cameron PL, Rakic P (1997) Developmental expression, pattern of distribution, and effect on cell aggregation implicate a neuron-glial junctional domain protein in neuronal migration. J Comp Neurol 387:467–488.

Catlett NL, Weisman LS (1998) The terminal tail region of a yeast myosin-V mediates its attachment to vacuole membranes and sites of polarized growth. Proc Natl Acad Sci USA 95:14799–14804.

Chen Y-H, Xiang M, Alessi DR, Campbell DG, Shanahan C, Cohen P, Cohen PTW (1994) Molecular cloning of cDNA encoding the 110 kDa and 21 kDa regulatory subunits of smooth muscle protein phosphatase 1M. FEBS Lett 356:51–55.

Chen ZY, Hasson T, Kelley PK, Schwender BJ, Schwartz MF, Ramakrishnan M, Kimberling WJ, Mooseker MS, Corey DP (1996) Molecular cloning and domain structure of human myosin VIIA, the gene product defective in Usher syndrome 1B. Genomics 36:440–448.

Chieregatti E, Gartner A, Stöffler H-E, Bähler M (1998) Myr 7 is a novel myosin IX-RhoGAP expressed in rat brain. J Cell Sci 111:3597–3608.

Church GM, Gilbert W (1984) Genomic sequencing. Proc Natl Acad Sci USA 81:1991–1995.

Costa MC, Mani F, Santoro W, Espreafico EM, Larson RE (1999) Brain myosin-V, a calmodulin-carrying myosin, binds to calmodulin-dependent protein kinase II and activates its kinase activity. J Biol Chem 274:15811–15819.

DePina AS, Langford GM (1999) Vesicle transport: the role of actin filaments and myosin motors. Microsc Res Tech 47:93–106.

Egloff M-P, Johnson DF, Moorhead G, Cohen PTW, Cohen P, Barford D (1997) Structural basis for the recognition of regulatory subunits by the catalytic subunit of protein phosphatase 1. EMBO J 16:1876–1887.

Felsenstein J (1993) PHYLIP (Phylogeny Inference Package) version 3.5c. Program distributed by author. Department of Genetics, University of Washington, Seattle.

Fucini RV, Navarrete A, Vadakkan C, Lacomis L, Erdjument-Bromage H, Tempst P, Stamnes M (2000) Activated ADP-ribosylation factor assembles distinct pools of actin on Golgi membrane. J Biol Chem 275:18824–18829.

Fujioka M, Takahashi N, Odai H, Araki S, Ichikawa K, Feng J, Nakamura M, Kaibuchi K, Hartshorne DJ, Nakano T, Ito M (1998) A new isoform of human myosin phosphatase targeting/regulatory subunit (MYPT2): cDNA cloning, tissue expression, and chromosomal mapping. Genomics 49:59–68.

Gibson F, Walsh J, Mburu P, Varela A, Brown KA, Antonio M, Biesel KW, Steel KP, Brown SDM (1995) A type VII myosin encoded by the mouse deafness gene *shaker-1*. Nature 374:62–64.

Gleeson JG, Walsh CA (2000) Neuronal migration disorders: from genetic diseases to developmental mechanisms. Trends Neurosci 23:352–359.

Gorman SW, Haider NB, Grieshammer U, Swiderski RE, Kim E, Welch JW, Searby C, Leng S, Carmi R, Sheffield VC, Duhl DM (1999) The cloning and developmental expression of unconventional myosin IXA (MYO9A), a gene in the Bardet-Biedl Syndrome (BBS4) region at chromosome 15q22–q23. Genomics 59:150–160.

Goslin K, Banker G (1991) Rat hippocampal neurons in low-density culture. In: Culturing nerve cells (Banker G, Goslin K, eds), pp 251–281. Cambridge, MA: Bradford/MIT.

Grewal PK, Jones A-M, Maconochie MM, Lemmers RJF, Frants RR, Hewitt JE (1999) Cloning of the murine unconventional myosin gene *Myo9b* and identification of alternative splicing. Gene 240:389–398.

Hartshorne DJ (1998) Myosin phosphatase: subunits and interactions. Acta Physiol Scand 164:483–493.

Hasson T, Mooseker MS (1994) Porcine myosin-VI: characterization of a new mammalian unconventional myosin. J Cell Biol 127:425–440.

Hatten ME (1985) Neuronal regulation of astroglial morphology and proliferation in vitro. J Cell Biol 100:384–396.

Hatten ME (1999) Central nervous system migration. Annu Rev Neurosci 22:511–539.

Hayden,SM, Wolenski JS, Mooseker MS (1990) Binding of brush border myosin I to phospholipid vesicles. J Cell Biol 111:443–451.

Heidemann SR, Buxbaum RE (1998) Cell crawling: first the motor, now the transmission. J Cell Biol 141:1–4.

Hirano K, Phan BC, Hartshorne DJ (1997) Interactions of the subunits of smooth muscle myosin phosphatase. J Biol Chem 272:3683–3688.

Hodge T, Cope MJTV (2000) A myosin family tree. J Cell Sci 113:3353–3354.

Houdusse A, Silver M, Cohen C (1996) A model of Ca(2+)-free calmodulin binding to unconventional myosins reveals how calmodulin acts as a regulatory switch. Structure 4:1475–1490.

Huang JD, Cope MJTV, Mermall V, Strobe MC, Kendrick-Jones J, Russell LB, Mooseker MS, Copeland NG, Jenkins NA (1998a) Molecular genetic dissection of mouse unconventional myosin-VA: head region mutations. Genetics 118:1951–1961.

Huang JD, Mermall V, Strobel MC, Russell LB, Mooseker MS, Copeland NG, Jenkins NA (1998b) Molecular genetic dissection of mouse unconventional myosin-VA: tail region mutations. Genetics 118:1963–1972.

Hubbard MJ, Cohen P (1989) Regulation of protein phosphatase-1G from rabbit skeletal muscle. 1. Phosphorylation by cAMP-dependent protein kinase at site 2 releases catalytic subunit from the glycogen-bound holoenzyme. Eur J Biochem 186:701–709.

Hunkapiller MW, Lujan E, Ostrander F, Hood LE (1983) Isolation of

microgram quantities of proteins from polyacrylamide gels for amino acid sequence analysis. Methods Enzymol 91:227–236.
Johnson D, Cohen P, Chen MX, Chen YH, Cohen PTW (1997) Identification of the regions on the M110 subunit of protein phosphatase 1M that interact with the M21 subunit and with myosin. Eur J Biochem 244:931–939.
Kakita A, Goldman JE (1999) Patterns and dynamics of SVZ cell migration in the postnatal forebrain: monitoring living progenitors in slice preparations. Neuron 23:461–472.
Kelley PM, Weston MD, Chen ZY, Orten DJ, Hasson T, Overbeck LD, Pinnt J, Talmadge CB, Ing P, Mooseker MS, Corey D, Sumegi J, Kimberling WJ (1997) The genomic structure of the gene defective in Usher syndrome type Ib (MYO 7A). Genomics 40:73–79.
Kennedy MB (2000) Signal-processing machines at the postsynaptic density. Science 290:750–754.
Kozak M (1991) An analysis of vertebrate mRNA sequences: intimation of translational control. J Cell Biol 115:887–903.
Kuhar SG, Feng L, Vidan S, Ross ME, Hatten ME, Heintz N (1993) Changing patterns of gene expression define four stages of cerebellar granule neuron differentiation. Development 117:97–104.
Laemmli UK (1970) Cleavage of structural proteins during the assembly of the head of bacteriophage T4. Nature 227:680–685.
Lambert J, Naeyaert JM, Callens T, DePaepe A, Messiaen L (1998) Human myosin V gene produces different transcripts in a cell-specific manner. Biochem Biophys Res Commun 252:329–333.
Lauffenburger DA, Horwitz AF (1996) Cell migration: a physically integrated molecular process. Cell 84:359–369.
Lee C, Levin A, Branton D (1987) Copper staining: a five-minute protein stain for sodium dodecyl sulfate-polyacrylamide gels. Anal Biochem 166:308–312.
Levison SW, Goldman JE (1993) Both oligodendrocytes and astrocytes develop from progenitors in the subventricular zone of postnatal rat forebrain. Neuron 10:201–212.
Levison SW, McCarthy KD (1991) Astroglia in culture. In: Culturing nerve cells (Banker G, Goslin, K, eds), pp 309–336. Cambridge, MA: Bradford/MIT.
Liang Y, Wang A, Belyantseva IA, Anderson DW, Probst FJ, Barber TD, Miller W, Touchman JW, Jin L, Sullivan SL, Sellers JR, Camper SA, Lloyd RV, Kachar B, Friedman TB, Fridell RA (1999) Characterization of the human and mouse unconventional myosin XV genes responsible for hereditary deafness *DFNB3* and Shaker 2. Genomics 61:243–258.
Liu XZ, Walsh J, Mburu P, Kendrick-Jones J, Cope MJTV, Steel KP, Brown SDM (1997a) Mutations in the myosin VIIA gene cause nonsyndromic recessive deafness. Nat Genet 16:188–190.
Liu XZ, Walsh J, Tamagawa Y, Kitamura K, Nishizawa M, Steel KP, Brown SDM (1997b) Autosomal dominant non-syndromic deafness caused by a mutation in the myosinb VIIA gene. Nat Genet 17:268–269.
Machesky LM, Insall RH (1999) Signaling to actin dynamics. J Cell Biol 146:267–272.
MacMillan LB, Bass MA, Cheng N, Howard EF, Tamura M, Strack S, Wadzinski BE, Colbran RJ (1999) Brain actin-associated protein phosphatase 1 haloenzymes containing spinophilin, neurabin, and selected catalytic subunit isoforms. J Biol Chem 274:35845–35854.
Mburu P, Liu XZ, Walsh J, Saw D, Cope MJTV, Gibson F, Kendrick-Jones J, Steel KP, Brown SDM (1997) Mutation analysis of the mouse myosin VIIA deafness gene. Genes Funct 1:191–203.
McAvoy T, Allen PB, Obaishi H, Nakanishi H, Takai Y, Greengard P, Nairn AC, Hemmings HC (1999) Regulation of neurabin I interaction with protein phosphatase 1 by phosphorylation. Biochemistry 38:12943–12949.
Mermall V, Post PL, Mooseker MS (1998) Unconventional myosins in cell movement, membrane traffic, and signal transduction. Science 279:527–533.
Michaely P, Bennett V (1992) The ANK repeat: a ubiquitous motif involved in macromolecular recognition. Trends Cell Biol 2:127–129.
Mitchison TJ, Cramer LP (1996) Actin-based cell motility and cell locomotion. Cell 84:371–379.
Montell C, Rubin GH (1988) The *Drosophila* ninaC locus encodes two photoreceptor cell-specific proteins with domains homologous to protein kinases and the myosin heavy chain head. Cell 52:757–772.
Mooseker MS, Cheney RE (1995) Unconventional myosins. Annu Rev Cell Dev Biol 11:633–675.
Mount SM (1982) A catalogue of splice junction sequences. Nucleic Acids Res 10:459–472.
Müller RT, Honnert U, Reinhard J, Bähler M (1997) The rat myosin myr 5 is a GTPase-activating protein for rho in vivo: essential role of arginine 1695. Mol Biol Cell 8:2039–2053.
Nagase T, Ishikawa K-I, Suyama M, Kikuno R, Hirosawa M, Miyajima N, Tanaka A, Kotani H, Nomura N, Ohara O (1998) Prediction of the coding sequences of unidentified human genes. XII. The complete sequences of 100 new cDNA clones from brain which code for large proteins in vitro. DNA Res 5:355–364.
Nakanishi H, Obaishi H, Satoh A, Wada M, Mandai K, Satoh K, Nishioka H, Matsuura Y, Mizoguchi A, Takai Y (1997) Neurabin: a novel neural tissue-specific actin filament-binding protein involved in neurite formation. J Cell Biol 139:951–961.
Ng KP, Kambara T, Matsuura M, Burke M, Ikebe M (1996) Identification of Myosin III as a protein kinase. Biochemistry 35:9392–9399.
O'Rourke N, Chenn A, McConnell S (1997) Postmitotic neurons migrate tangentially in the cortical ventricular zone. Development 124:997–1005.
Ouimet CC, da Cruz e Silva EF, Greengard P (1995) The α and γ1 isoforms of protein phosphatase 1 are highly and specifically concentrated in dendritic spines. Proc Natl Acad Sci USA 92:3396–3400.
Pastural E, Barrat FJ, Dufourcq-Lagelouse R, Certain S, Sanal O, Jabado N, Seger R, Griscelli C, Fischer A, Saint Basile G (1997) Griscelli disease maps to chromosome 15q21 and is associated with mutations in the myosin-Va gene. Nat Genet 16:289–292.
Pawson T, Scott JD (1997) Signaling through scaffold, anchoring, and adaptor proteins. Science 278:2075–2080.
Porter JA, Hicks JL, Williams DS, Montell C (1992) Differential localizations of and requirements for the two *Drosophila* ninaC kinase/myosins in photoreceptor cells. J Cell Biol 683–693.
Prehoda KE, Do JL, Lim WA (1999) Structure of the Enabled/VASP homology 1 domain-peptide complex: a key component in the spatial control of actin assembly. Cell 97:471–480.
Price NE, Mumby MC (1999) Brain protein serine/threonine phosphatases. Curr Opin Neurobiol 9:336–342.
Probst FJ, Fridell RA, Raphael Y, Saunders TL, Wang A, Liang Y, Morell RJ, Touchman JW, Lyons RH, Noben-Trauth K, Friedman TB, Camper SA (1998) Correction of deafness in shaker-2 mice by an unconventional myosin in a BAC transgene. Science 280:1444–1447.
Rakic P (1990) Principles of neural cell migration. Experientia 46:882–891.
Reck-Peterson SL, Novick PJ, Mooseker MS (1999) The tail of a yeast class V myosin, Myo2p, functions as a localization domain. Mol Biol Cell 10:1001–1017.
Reiner O (2000) LIS1: Let's interact sometimes (Part 1). Neuron 28:633–636.
Reinhard J, Scheel AA, Diekmann D, Hall A, Ruppert C, Bähler M (1995) A novel type of myosin implicated in signalling by rho family GTPases. EMBO J 14:697–704.
Ruppert C, Kroschewski R, Bähler M (1993) Identification, characterization and cloning of myr 1, a mammalian myosin-1. J Cell Biol 120:1393–1403.
Schluter K, Jockusch BM, Rothkegel M (1997) Profilins as regulators of actin dynamics. Biochim Biophys Acta 1359:97–109.
Schneider C, Newman RA, Sutherland DR, Asser U, Greaves MF (1982) A one step purification of membrane proteins using a high efficiency immunomatrix. J Biol Chem 257:10766–10769.
Schott D, Ho J, Pruyne D, Bretscher A (1999) The COOH-terminal domain of Myo2p, a yeast myosin V, has a direct role in secretory vesicle targeting. J Cell Biol 147:791–807.
Sherr EH, Joyce MP, Greene LA (1993) Mammalian myosin Iα, Iβ, and Iγ: new widely expressed genes of the myosin I family. J Cell Biol 120:1405–1416.
Shimizu H, Ito M, Miyahara M, Ichikawa K, Okubo S, Konishi T, Naka M, Tanaka T, Hirano K, Hartshorne DJ, Nakano T (1994) Characterization of the myosin-binding subunit of smooth muscle phosphatase. J Biol Chem 269:30407–30411.
Sidman RL, Rakic P (1973) Neuronal migration with special reference to developing human brain: a review. Brain Res 62:1–35.
Sokac AM, Bement WM (2000) Regulation and expression of metazoan unconventional myosins. Int Rev Cytol 200:197–304.
Solc CK, Derfler BH, Duyk GM, Corey DP (1994) Molecular cloning of myosins from the bullfrog saccular macula: a candidate for the hair cell adaption motor. Aud Neurosci 1:63–75.
Song HJ, Poo MM (2001) The cell biology of neuronal navigation. Nat Cell Biol 3:E81–E88.
Stöffler H-E, Honnert U, Bauer CA, Hofer D, Schwarz H, Muller RT, Drenckhahn D, Bähler M (1995) A novel mammalian myosin I from rat with an SH3 domain localizes to Con A-inducible, F-actin-rich structures at cell-cell contacts. J Cell Biol 129:819–830.
Strack S, Kini S, Ebner FF, Wadzinski BE, Colbran RJ (1999) Differential cellular and subcellular localization of protein phosphatase 1 isoforms in brain. J Comp Neurol 413:373–384.
Suetsugu S, Miki H, Takenawa T (1998) The essential role of profilin in the assembly of actin for microspike formation. EMBO J 17:6516–6526.
Suter DM, Forscher P (1998) An emerging link between cytoskeletal dynamics and cell adhesion molecules in growth cone guidance. Curr Opin Neurobiol 8:106–116.
Tanaka E, Sabry J (1995) Making the connection: cytoskeletal rearrangements during growth cone guidance. Cell 83:171–176.
Toth A, Kiss E, Gergely P, Walsh MP, Hartshorne DJ, Erdodi F (2000) Phosphorylation of MYPT1 by protein kinase C attenuates interaction with PP1 catalytic subunit and the 20 kDa light chain of myosin. FEBS Lett 484:113–117.
Towbin H, Staehlin T, Gordin J (1979) Electrophoretic transfer of pro-

teins from polyacrylamide gels to nitrocellulose sheets: procedures and some applications. Proc Natl Acad Sci USA 76:4350–4354.

Tsakraklides V, Krogh K, Wang L, Bizario JCS, Larson RE, Espreafico EM, Wolenski JS (1999) Subcellular localization of GFP-myosin-V in live mouse melanocytes. J Cell Sci 112:2853–2865.

Valderrama F, Luna A, Babia T, Martinez-Menarguez JA, Ballesta J, Barth H, Chaponnier C, Renau Piqueras J, Egea G (2000) The Golgi-associated COP1-coated buds and vesicles contain β/γ-actin. Proc Natl Acad Sci USA 97:1560–1565.

Wang A, Liang Y, Fridell RA, Probst FJ, Wilcox ER, Touchman JW, Morton CC, Morell RJ, Noben-Trauth K, Camper SA, Friedman TB (1998) Association of unconventional myosin MYO15 mutations with human nonsyndromic deafness DFNB3. Science 280:1447–1451.

Weil D, Blanchard S, Kaplan J, Guilford P, Gibson F, Walsh J, Mbruru P, Valera A, Levilliers J, Weston MD, Kelley PM, Levi-Acobas F, Larget-Piet D, Munnich A, Steel KP, Kimberling WJ, Brown SDM, Petit C (1995) Defective myosin VIIA gene responsible for Usher syndrome type 1B. Nature 374:60–61.

Weil D, Kussel P, Blanchard S, Levy G, Levi-Acobas F, Drira M, Ayadi H, Petit C (1997) The autosomal recessive isolated deafness, DFNB2, and the Usher 1B syndrome are allelic defects of the myosin-VIIA gene. Nat Genet 16:191–193.

Wichterle H, Garcia-Verdugo JM, Alvarez-Buylla A (1997) Direct evidence for homotypic, glia- independent neuronal migration. Neuron 18:779–791.

Wirth JA, Jensen KA, Post PL, Bement WM, Mooseker MS (1996) Human myosin IX-b. An unconventional myosin with a chimerin-like rho/rac GTPase-activating protein domain in its tail. J Cell Sci 109:653–661.

Zerlin M, Levison SW, Goldman JE (1995) Early patterns of migration, morphogenesis, and intermediate filament expression of subventricular zone cells in the postnatal rat forebrain. J Neurosci 15:7238–7249.

Zhu Y, Li HS, Zhou L, Wu JY, Rao Y (1999) Cellular and molecular guidance of GABAergic neuronal migration from an extracortical origin to the neocortex. Neuron 23:473–485.